REFERENCES

[1] NORDE´N, A.R.A.B. Peptide nucleic acid (PNA): its medical and biotechnical applications and promise for the future. The FASEB Journal. 14 (2000): 1041-1060.

[2] Gros, E., and others. A non-covalent peptide-based strategy for protein and peptide nucleic acid transduction. Biochimica et Biophysica Acta - Biomembranes. (2006): 384-393.

[3] Nielsen, P.E. and Egholm, M. An introduction to peptide nucleic acid. Current Issues in Molecular Biology. (1999): 89-104.

[4] Hanson, C.L. and Robinson, C.V. Protein-nucleic acid interactions and the expanding role of mass spectrometry. Journal of Biological Chemistry. (2004): 24907-24910.

[5] Nielsen, P.E. Peptide nucleic acids (PNA) in chemical biology and drug discovery. Chemistry and Biodiversity. (2010): 786-804.

[6] Taechalertpaisarn, J. and others. DNA-, RNA- and self-pairing properties of a pyrrolidinyl peptide nucleic acid with a (2′R,4′S)-prolyl-(1S,2S)-2-aminocyclopentanecarboxylic acid backbone. Tetrahedron Letters. (2010): 5822-5826.

[7] Bruce Armitage, T.K., Frydenlund, H., Rum, H. and Schuster, G.B. Peptide nucleic acid (PNA)/DNA hybrid duplexes: intercalation by an internally linked anthraquinone. Nucleic Acids Research. (1998): 715-720.

[8] Loo, J.A. Studying noncovalent protein complexes by electrospray ionization mass spectrometry. Mass Spectrometry Reviews. (1997): 1-23.

[9] Nielsen, B.H.a.P.E. Peptide nucleic acids (PNA): synthesis, properties and potential applications. Bioorganic & Medicinal Chemistry. (1996): 5-23.

[10] Baker, E.S. and Bowers, M.T. B-DNA helix stability in a solvent-free environment. Journal of the American Society for Mass Spectrometry. (2007): 1188-1195.

[11] Erin Shammel Baker, J.W.H., Gaylord, B.S., Bazan, G.C. and Bowers, M.T. PNA/dsDNA complexes: site specific binding and dsDNA biosensor applications. American Chemical Society. (2006): 8484-8492.

[12] Wan, K.X., Shibue, T., and Gross, M.L. Non-covalent complexes between DNA-binding drugs and double-stranded oligodeoxynucleotides: A study by ESI ion-

trap mass spectrometry. Journal of the American Chemical Society. (2000): 300-307.

[13] Huang, B., Hou, J., Lin, S., Chen, J., and Hong, H. Development of a PNA probe for the detection of the toxic dinoflagellate Takayama pulchella. Harmful Algae. (2008): 495-503.

[14] Banerjee, A. and Kumar, V.A. C3'-endo-puckered pyrrolidine containing PNA has favorable geometry for RNA binding: Novel ethano locked PNA (ethano-PNA). Bioorganic & Medicinal Chemistry. (2013): 4092-4101.

[15] Veenstra, T.D. Electrospray Ionization Mass Spectrometry: A promising new technique in the study of protein/DNA noncovalent complexes. Biochemical and Biophysical Research Communications. (1999): 1-5.

[16] Galefn, D.C. and Smithcor, R.D. Characterization of noncovalent complexes formed between minor groove binding molecules and duplex DNA by electrospray ionization-mass spectrometry. Journal of the American Society for Mass Spectrometry. (1995): 1154-1164.

[17] Wortmann, A., Jecklin, M.C., Touboul, D., Badertscher, M., and Zenobi, R. Binding constant determination of high-affinity protein-ligand complexes by electrospray ionization mass spectrometry and ligand competition. Journal of Mass Spectrometry. (2008): 600-608.

[18] Heuer-Jungemann, A., Howarth, N.M., Ja'Afaru, S.C., and Rosair, G.M. Development of a convenient route for the preparation of the N2-Cbz-protected guaninyl synthon required for Boc-mediated PNA synthesis. Tetrahedron Letters. (2013): 6275-6278.

[19] Brandt, O. and Hoheisel, J.D. Peptide nucleic acids on microarrays and other biosensors. Trends in Biotechnology. (2004): 617-622.

[20] Arlinghaus, H.F., Schröder, M., Feldner, J.C., Brandt, O., Hoheisel, J.D., and Lipinsky, D. Development of PNA microarrays for gene diagnostics with TOF-SIMS. Applied Surface Science. (2004): 392-396.

[21] Warrens, A.N., Jones, M.D., and Lechler, R.I. Splicing by overlap extension by PCR using asymmetric amplification: an improved technique for the generation of hybrid proteins of immunological interest. Gene. (1997): 29-35.

[22] Benkestock, K. Electrospray ionization mass spectrometry for determination of noncovalent interactions in drug discovery. Doctoral dissertation, School of Chemical Science and Engineering Royal Institute of Technology Stockholm, (2008).

[23] Goodlett, R.A.a.D.R. Mass spectrometry in proteomics. American Chemical Society. (2001): 269-295.

[24] Zhang, S., Van Pelt, C.K., and Wilson, D.B. Quantitative determination of noncovalent binding interactions using automated nanoelectrospray mass spectrometry. Analytical Chemistry. (2003): 3010-3018.

[25] Daniel, J.M., Friess, S.D., Rajagopalan, S., Wendt, S., and Zenobi, R. Quantitative determination of noncovalent binding interactions using soft ionization mass spectrometry. International Journal of Mass Spectrometry. (2002): 1-27.

[26] Kharlamova, A., Prentice, B.M., Huang, T.Y., and McLuckey, S.A. Electrospray droplet exposure to gaseous acids for reduction of metal counter-ions in nucleic acid ions. International Journal of Mass Spectrometry. (2011): 158-166.

[27] Valérie, G. Electrospray mass spectrometry of noncovalent complexes between small molecule ligands and nucleic acids. Mass spectrometry of nucleosides and nucleic acids. (2010): 283-302.

[28] Rosu, F., De Pauw, E., and Gabelica, V. Electrospray mass spectrometry to study drug-nucleic acids interactions. Biochimie. (2008): 1074-1087.

[29] Hiraoka, K. Fundamentals of mass spectrometry. Springer New York Heidelberg Dordrecht London, 2013.

[30] Chen, Z. and Weber, S.G. Determination of binding constants by affinity capillary electrophoresis, electrospray ionization mass spectrometry and phase-distribution methods. TrAC - Trends in Analytical Chemistry. (2008): 738-748.

[31] Jørgensen, T.J.D., Delforge, D., Remacle, J., Bojesen, G., and Roepstorff, P. Collision-induced dissociation of noncovalent complexes between vancomycin antibiotics and peptide ligand stereoisomers: Evidence for molecular recognition in the gas phase. International Journal of Mass Spectrometry. (1999): 63-85.

[32] Gajjela Raju, R.S., Reddy, V.S., Idris, M.M., Kamal, A. and Nagesh, N. Interaction of Pyrrolobenzodiazepine (PBD) Ligands with Parallel Intermolecular G-Quadruplex Complex Using Spectroscopy and ESI-MS. PLoS ONE. (2012).

[33] Casagrande, V., Alvino, A., Bianco, A., Ortaggi, G., and Franceschin, M. Study of binding affinity and selectivity of perylene and coronene derivatives towards duplex and quadruplex dma by ESI-MS. Journal of Mass Spectrometry. (2009): 530-540.

[34] Seonghee Ahn, J.R., Grigorean, G. and Lebrilla, C.B. Chiral Recognition in Gas-Phase Cyclodextrin: Amino Acid Complexes—Is the Three Point Interaction Still Valid in the Gas Phase. Journal of the American Society for Mass Spectrometry. (2001): 278-287.

[35] Deshayes, S., Morris, M., Heitz, F., and Divita, G. Delivery of proteins and nucleic acids using a non-covalent peptide-based strategy. Advanced Drug Delivery Reviews. (2008): 537-547.

[36] Flora, J.W., Shillady, D.D., and Muddiman, D.C. An experimental and theoretical study of the gas-phase decomposition of monoprotonated peptide nucleic acids. Journal of the American Society for Mass Spectrometry. (2000): 615-625.

[37] Riffet, V., Bourcier, S., and Bouchoux, G. Gas-phase basicity and acidity of tryptophan. International Journal of Mass Spectrometry. (2012): 47-56.

[38] Christopher Becker, F.A.F.-L., Gillig, K.G., Russell, W.K., Cologna, S.M. and Russell, D.H. A novel approach to collision-induced dissociation (CID) for ion mobility-mass spectrometry experiments. American Society for Mass Spectrometry. (2009): 907-914.

[39] Alice Delvolvé, J.-C.T., Bregant, S., Afonso, C., Burlina, F. and Fournier, F.O. Charge dependent behavior of PNA/DNA/PNA triplexes in the gas phase. Journal of Mass Spectrometry. (2006): 1498-1508.

[40] Ho, Y.H., Chen, J.W., and Hu, T.L. Elucidating factors manipulated the formation of multiply charged protein homomultimeric complexes by electrospray ionization. Journal of the Chinese Chemical Society. (2007): 391-400.

[41] Wu, Z., Gao, W., Phelps, M.A., Wu, D., Miller, D.D., and Dalton, J.T. Favorable Effects of weak acids on negative-ion electrospray ionization mass spectrometry. Analytical Chemistry. (2004): 839-847.

[42] Wan, K.X. Non-covalent complexes between DNA-binding drugs and double-stranded oligodeoxynucleotides: a study by ESI ion-trap mass spectrometry. Journal of the American Chemical Society. (2000): 300-307.

[43] Suparpprom, C., Srisuwannaket, C., Sangvanich, P., and Vilaivan, T. Synthesis and oligodeoxynucleotide binding properties of pyrrolidinyl peptide nucleic acids bearing prolyl-2-aminocyclopentanecarboxylic acid (ACPC) backbones. Tetrahedron Letters. (2005): 2833-2837.

[44] Vilaivan, C., and others. Pyrrolidinyl peptide nucleic acid with α/β-peptide backbone: A conformationally constrained PNA with unusual hybridization properties. Artificial DNA: PNA and XNA. (2011): 50-59.

[45] Pan, S., Sun, X., and Lee, J.K. Stability of complementary and mismatched DNA duplexes: Comparison and contrast in gas versus solution phases. International Journal of Mass Spectrometry. (2006): 238-248.

[46] Sebastian Tomac, M.S., Ratilainen, M., Wittung, P., Nielsen, P.E., Nordén, B. and Graislund, A. Ionic effects on the stability and conformation of peptide nucleic acid complexes. American Chemical Society. (1996): 5544-5552.

[47] Tatsuo Ohmichi, Y.K., Wu, P., Miyoshi, D., Karimata, H., and Sugimoto, N. DNA-based biosensor for monitoring pH in vitro and in living cells. Biochemistry. (2005): 7125-7130.

[48] Wittwer, C.T., Herrmann, M.G., Moss, A.A., and Rasmussen, R.P. Continuous fluorescence monitoring of rapid cycle DNA amplification. Biotechniques. (1997): 130-138.

[49] Wittwer, C.T., Ririe, K.M., Andrew, R.V., David, D.A., Gundry, R.A., and Balis, U.J. The lightCycler: a microvolume multisample fluorimeter with rapid temperature control. Biotechniques. (1997): 176-181.

[50] Bernard, P.S. and Wittwer, C.T. Real-time PCR technology for cancer diagnostics clin chem, (2000): 147-148.

APPENDIX

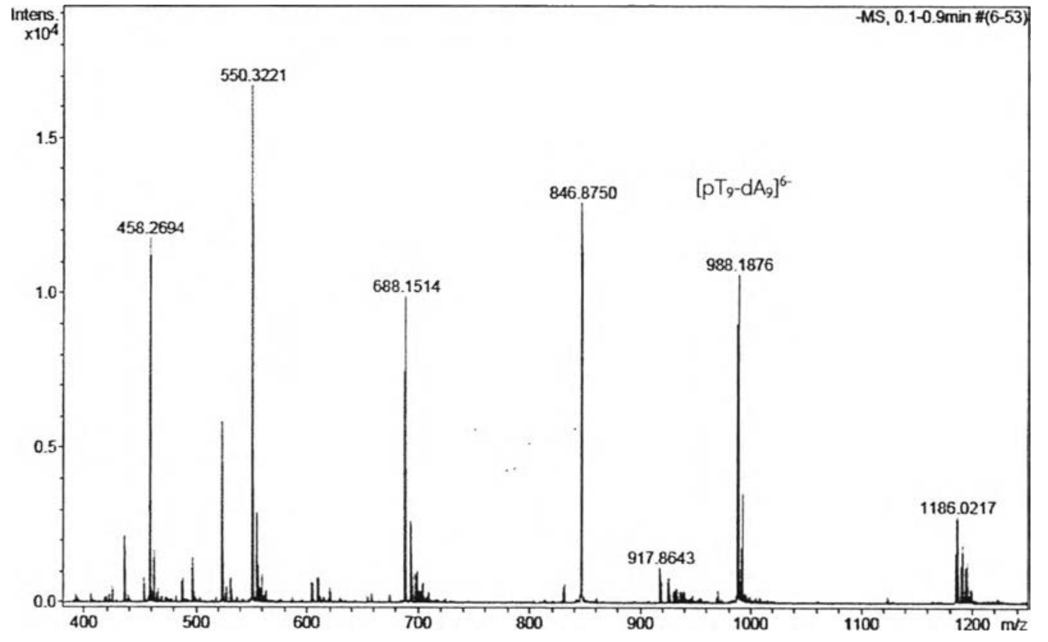

Figure A.1 Spectrum of duplex pT_9 – dA_9 at 0 eV.

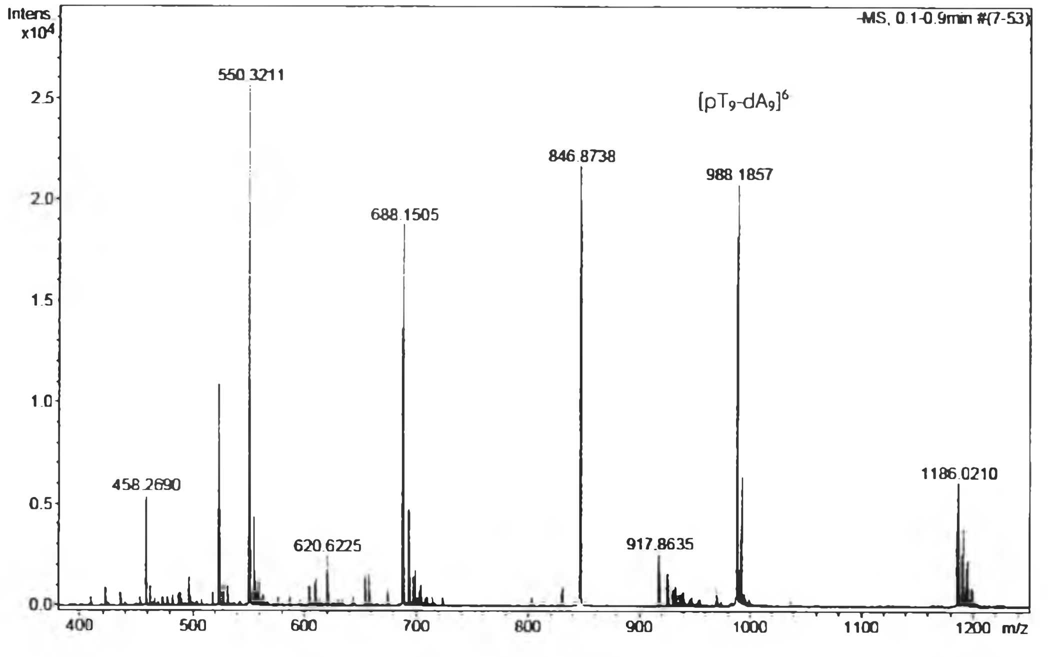

Figure A.2 Spectrum of duplex pT_9 – dA_9 at 2 eV.

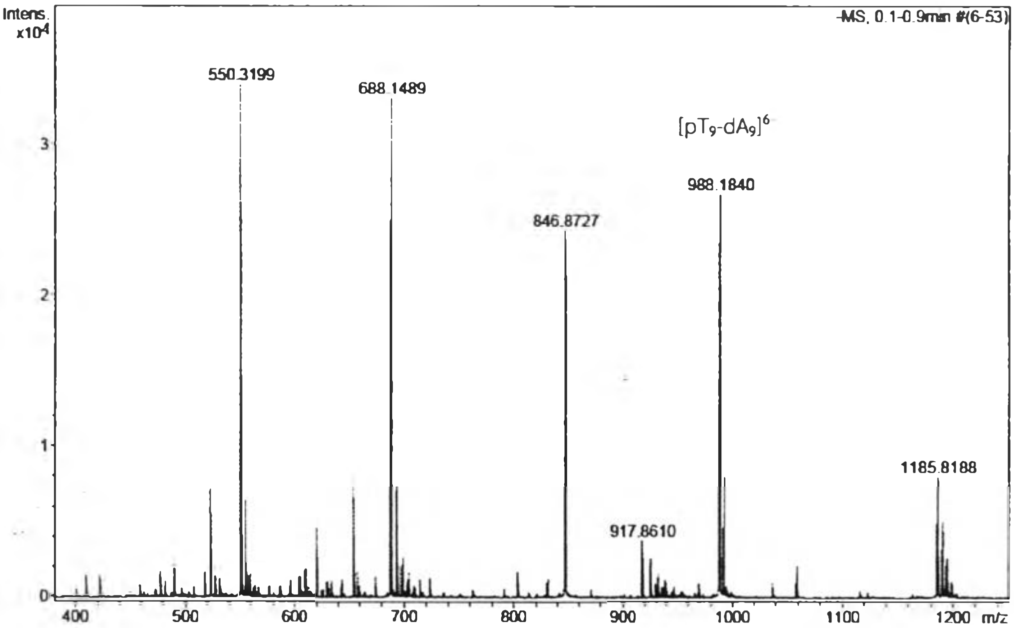

Figure A.3 Spectrum of duplex $pT_9 - dA_9$ at 4 eV.

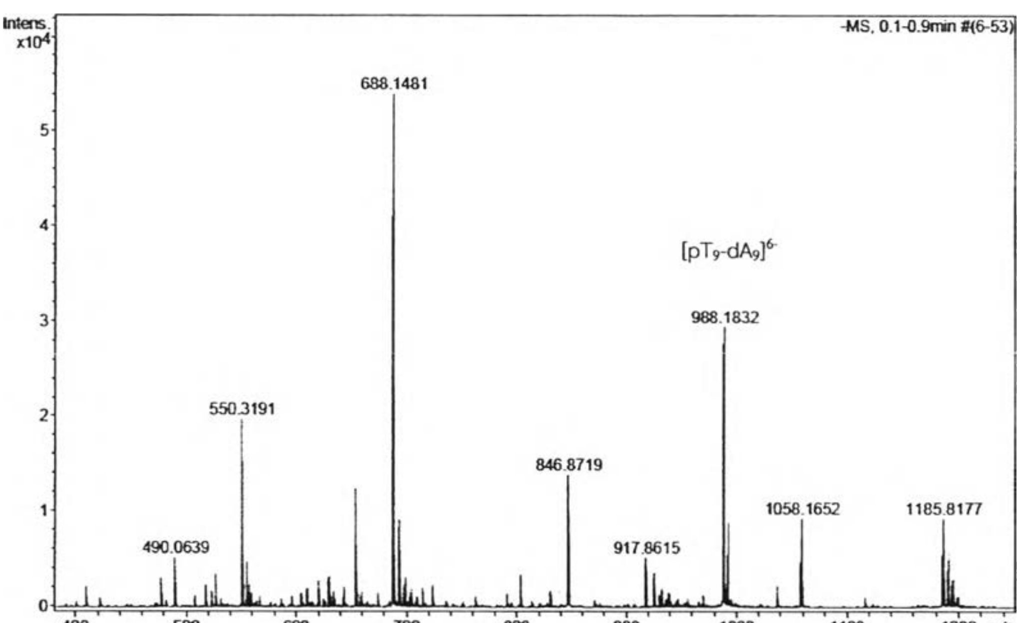

Figure A.4 Spectrum of duplex $pT_9 - dA_9$ at 6 eV.

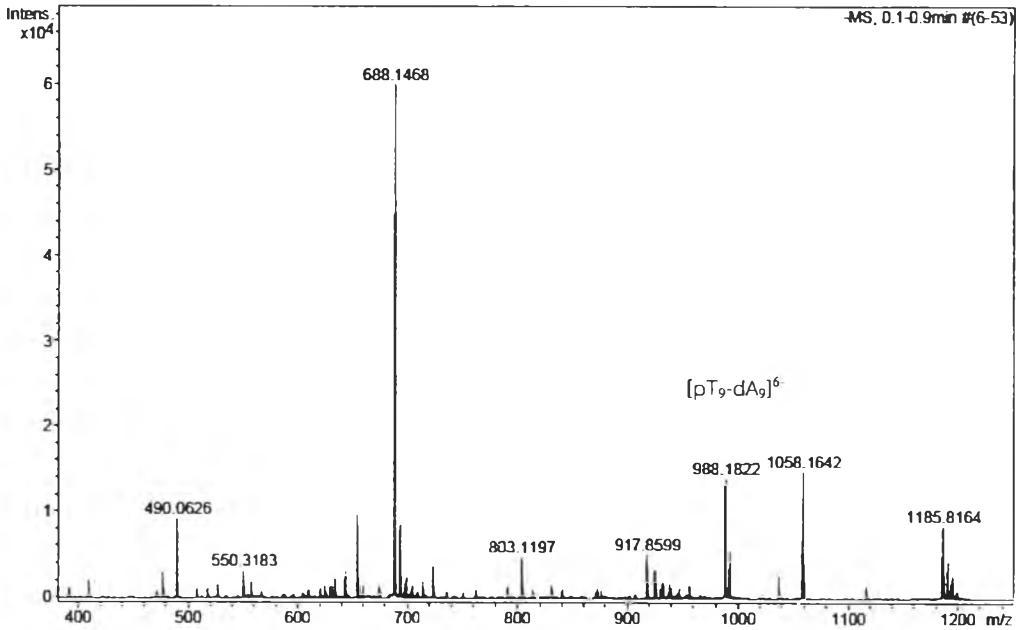

Figure A.5 Spectrum of duplex pT_9 – dA_9 at 8 eV.

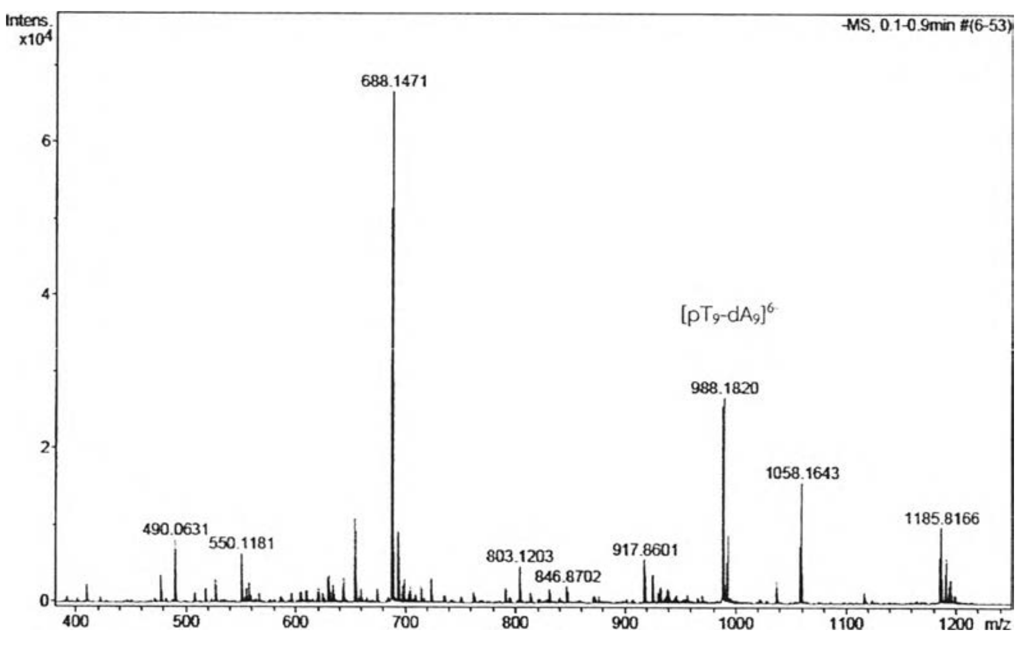

Figure A.6 Spectrum of duplex pT_9 – dA_9 at 10 eV.

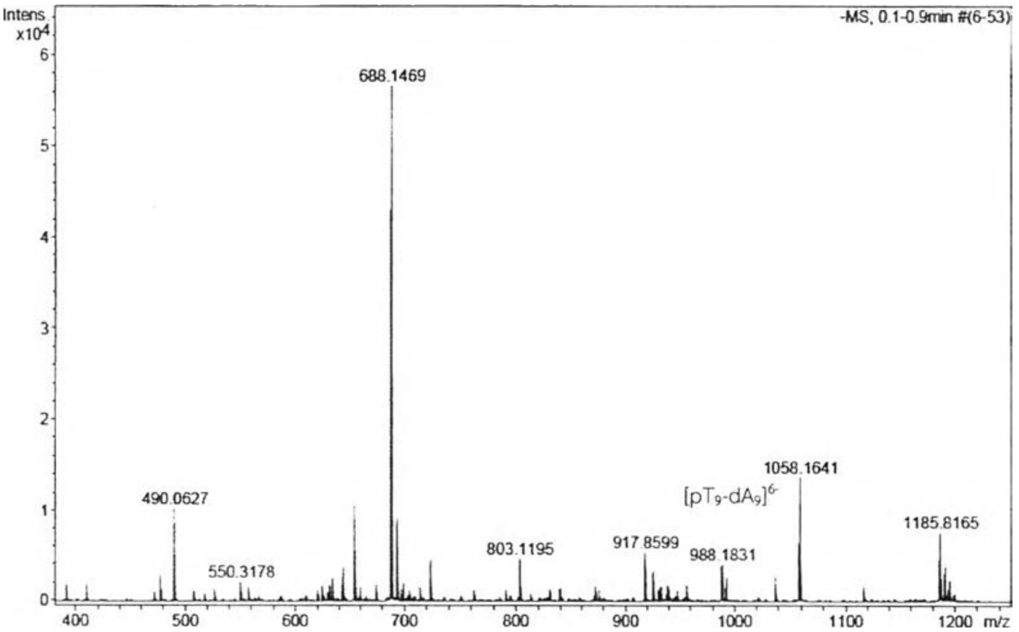

Figure A.7 Spectrum of duplex pT_9 – dA_9 at 12 eV.

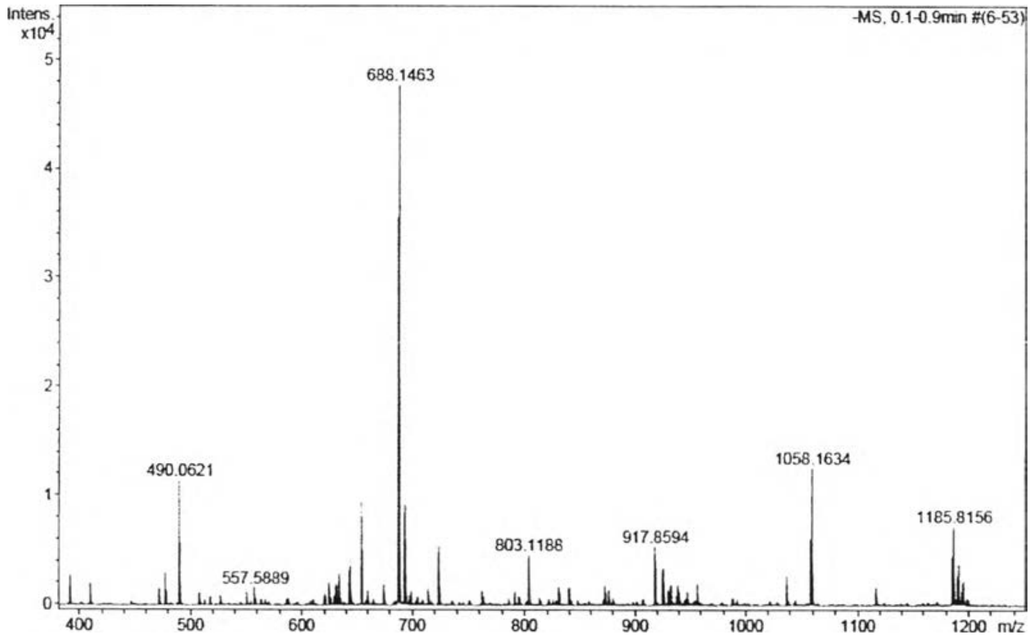

Figure A.8 Spectrum of duplex pT_9 – dA_9 at 14 eV.

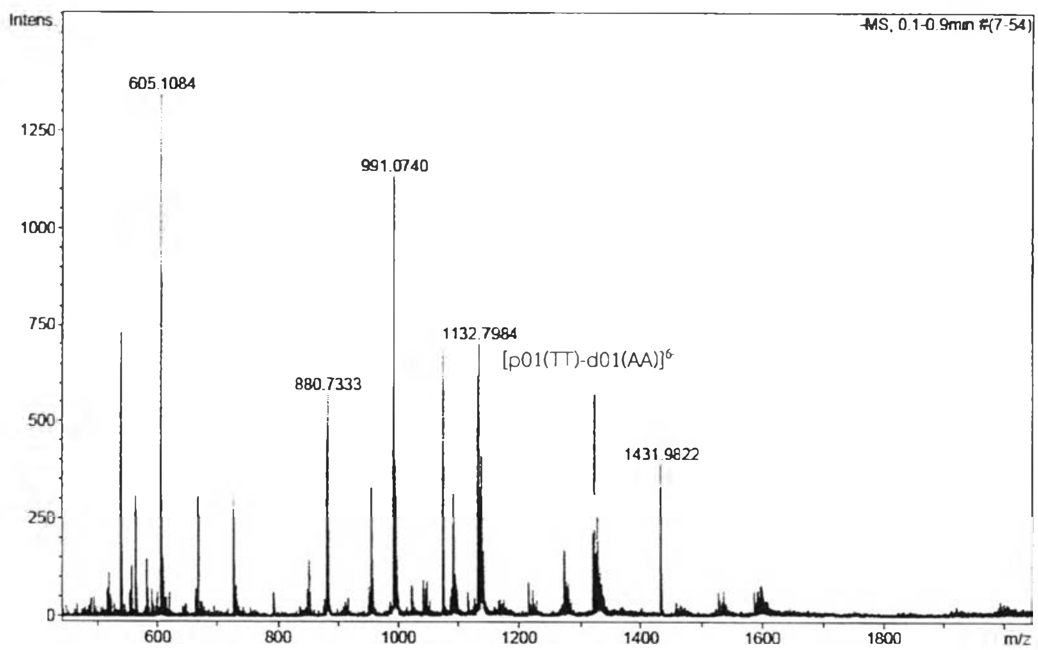

Figure A.9 Spectrum of duplex p01 (TT) - d01 (AA) at 0 eV.

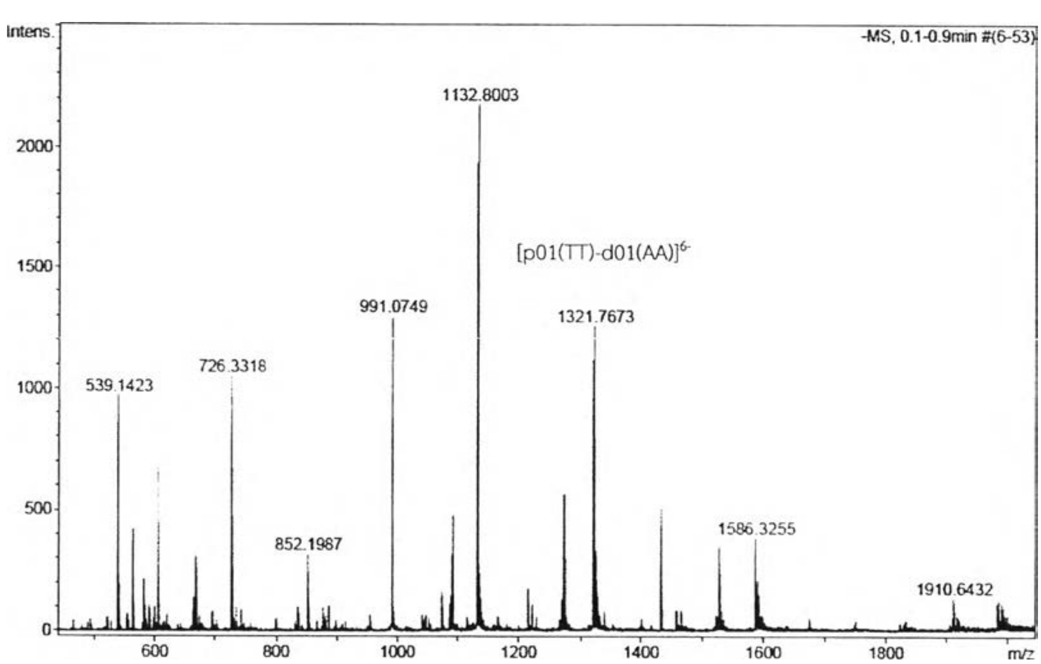

Figure A.10 Spectrum of duplex p01 (TT) - d01 (AA) at 2 eV.

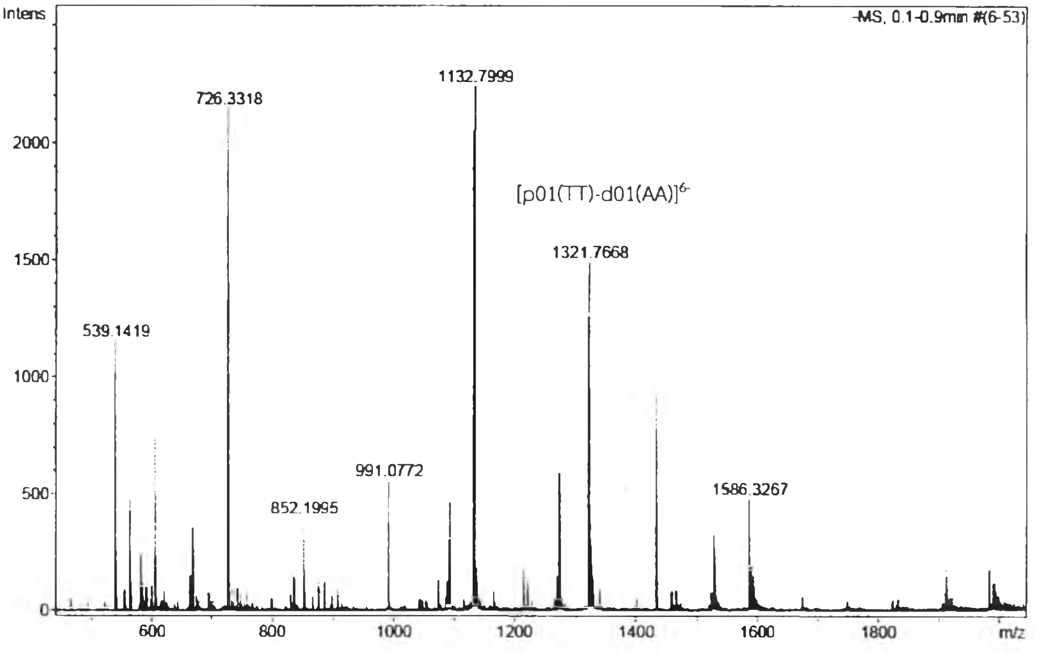

Figure A.11 Spectrum of duplex p01 (TT) - d01 (AA) at 4 eV.

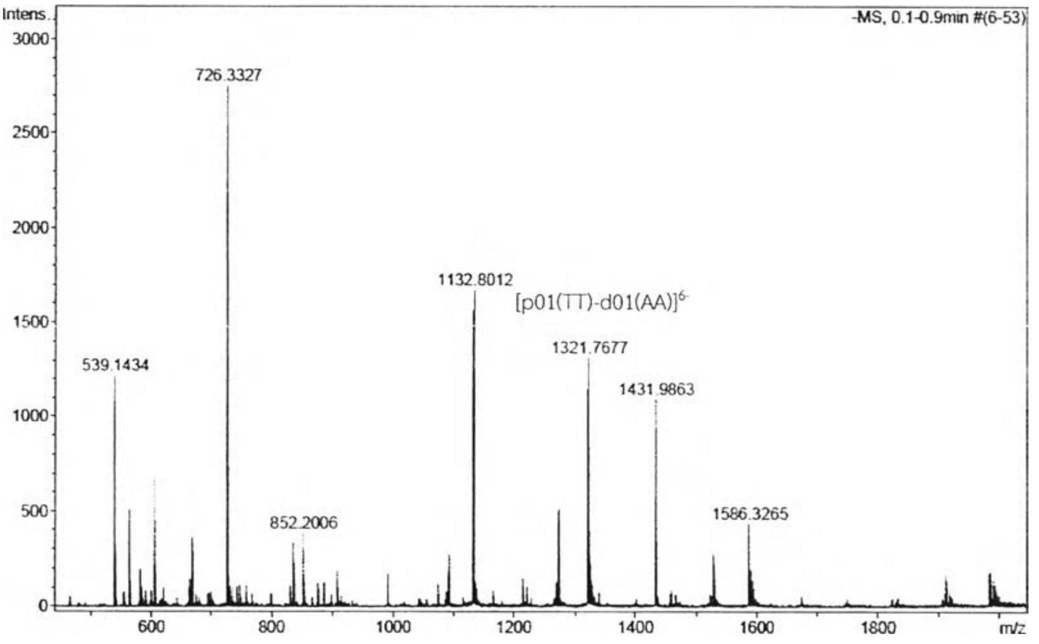

Figure A.12 Spectrum of duplex p01 (TT) - d01 (AA) at 6 eV.

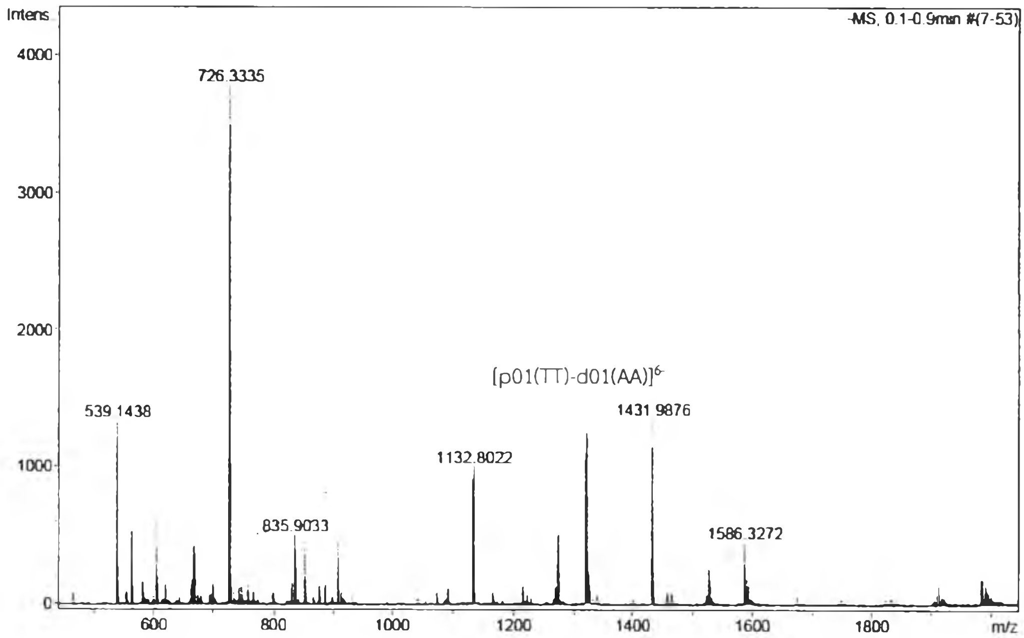

Figure A.13 Spectrum of duplex p01 (TT) - d01 (AA) at 8 eV.

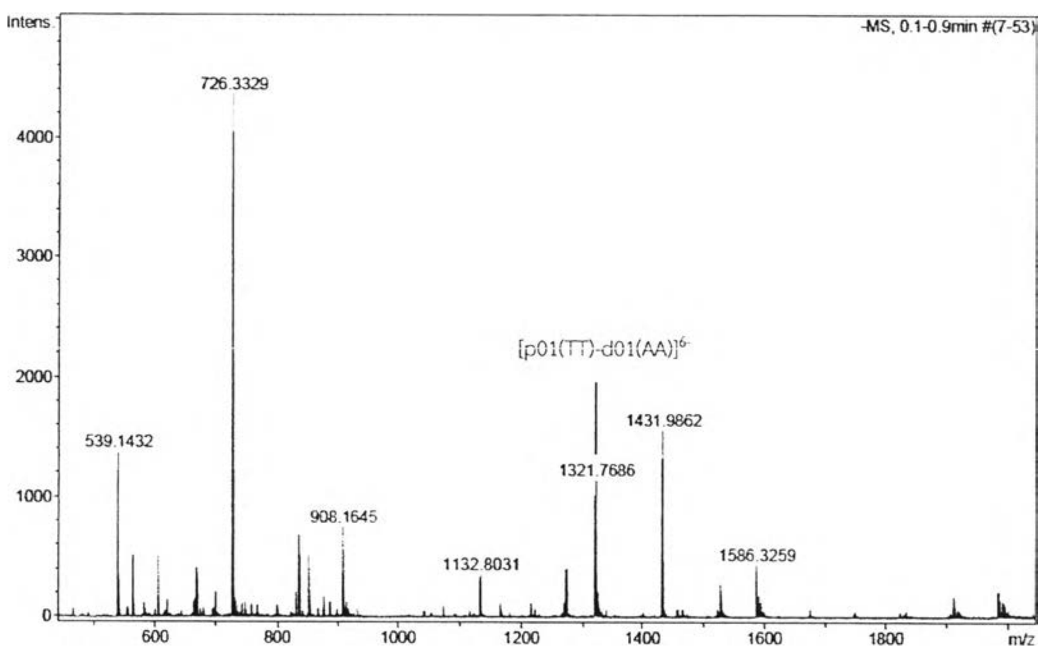

Figure A.14 Spectrum of duplex p01 (TT) - d01 (AA) at 10 eV.

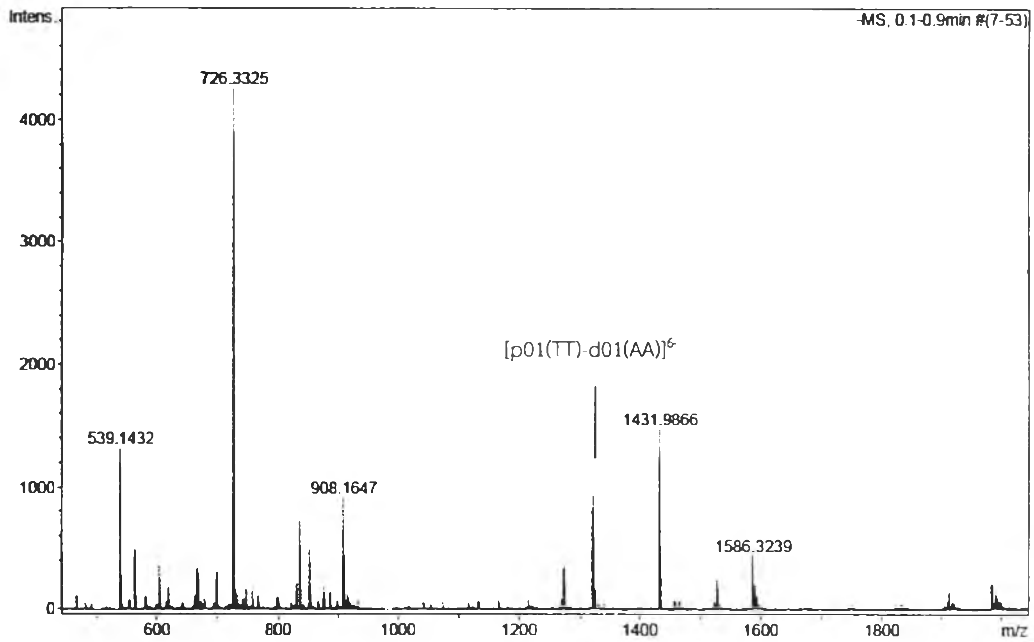

Figure A.15 Spectrum of duplex p01 (TT) - d01 (AA) at 12 eV.

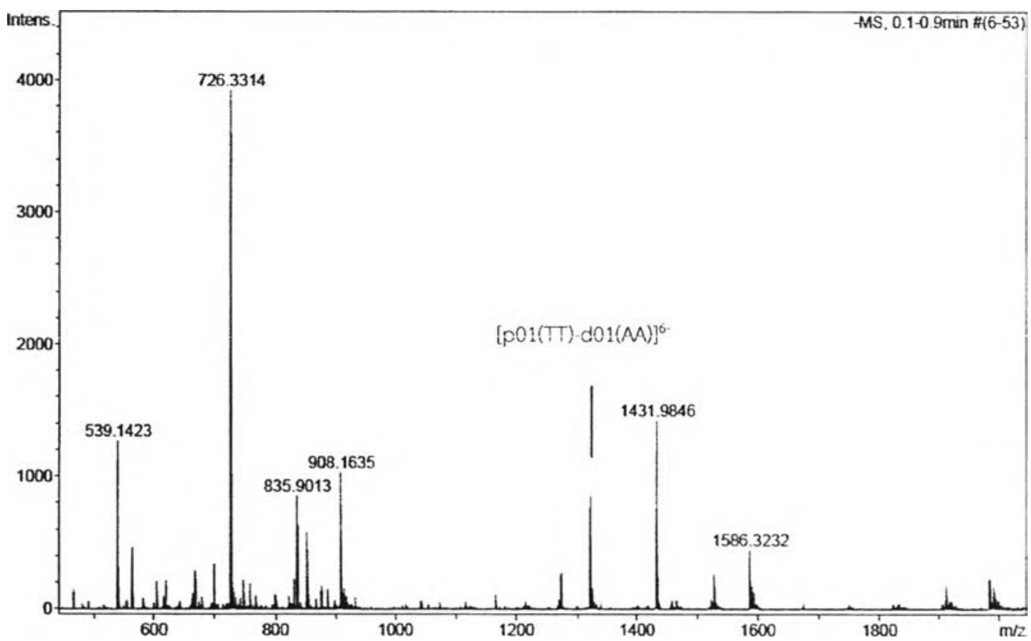

Figure A.16 Spectrum of duplex p01 (TT) - d01 (AA) at 14 eV.

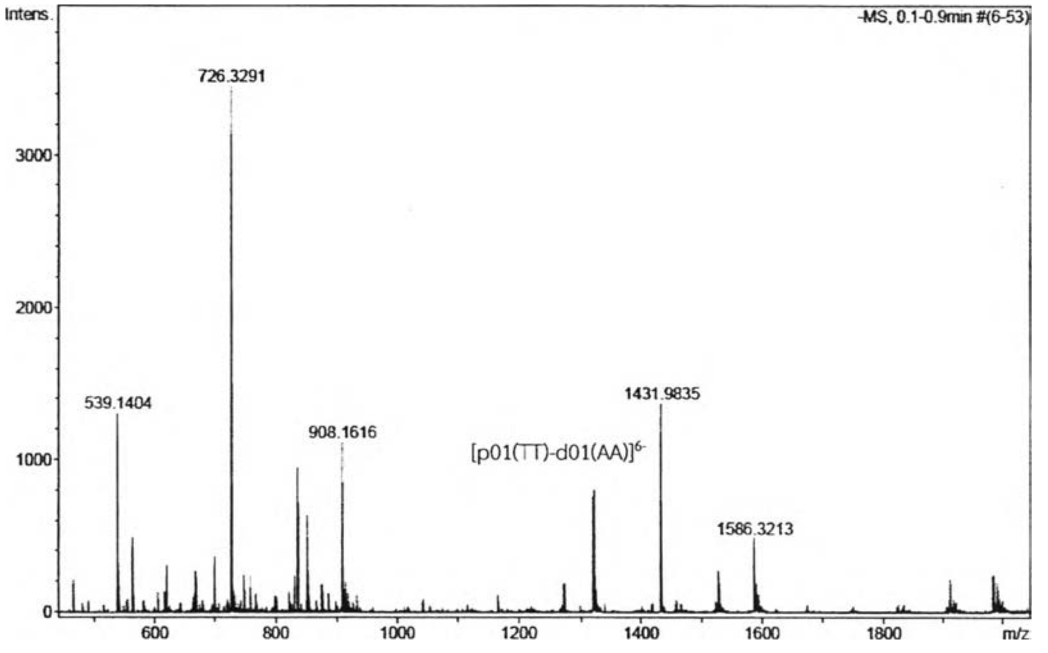

Figure A.17 Spectrum of duplex p01 (TT) - d01 (AA) at 16 eV.

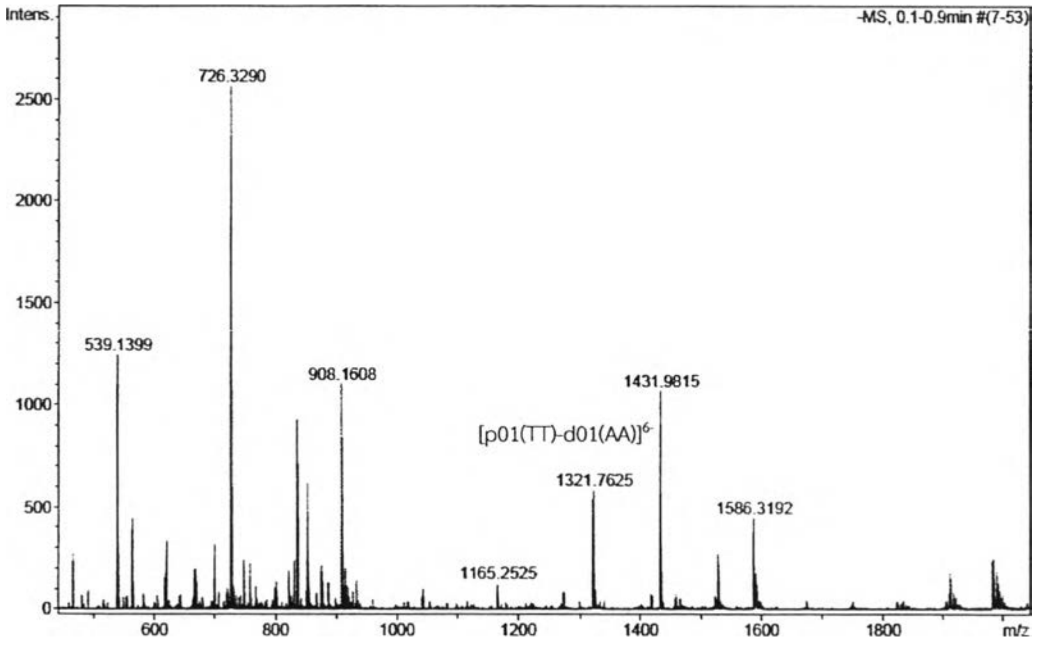

Figure A.18 Spectrum of duplex p01 (TT) - d01 (AA) at 18 eV.

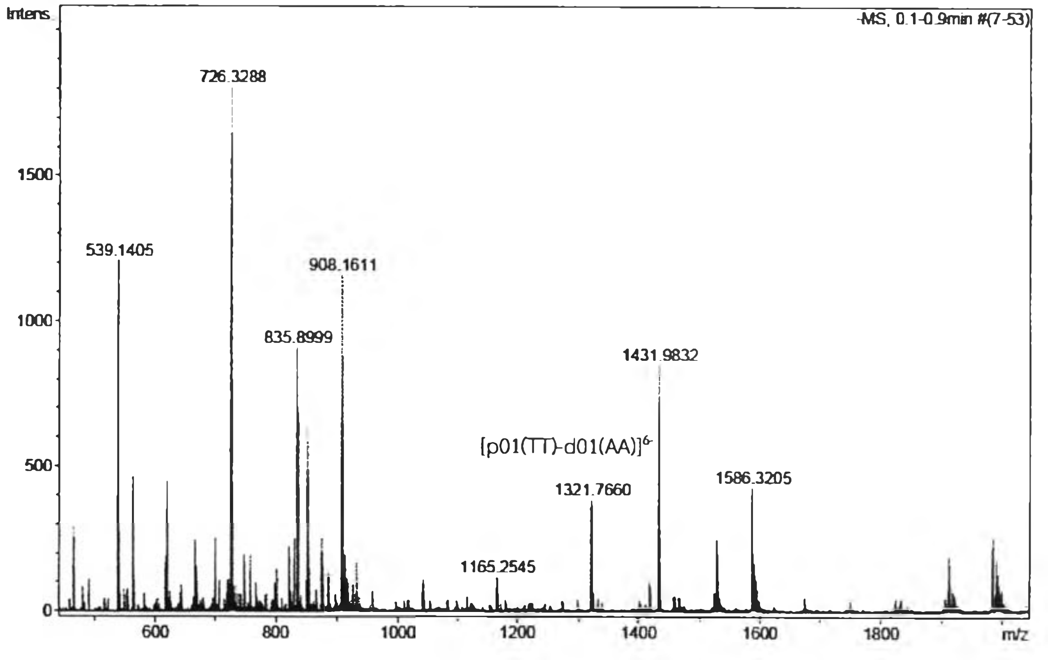

Figure A.19 Spectrum of duplex p01 (TT) - d01 (AA) at 20 eV.

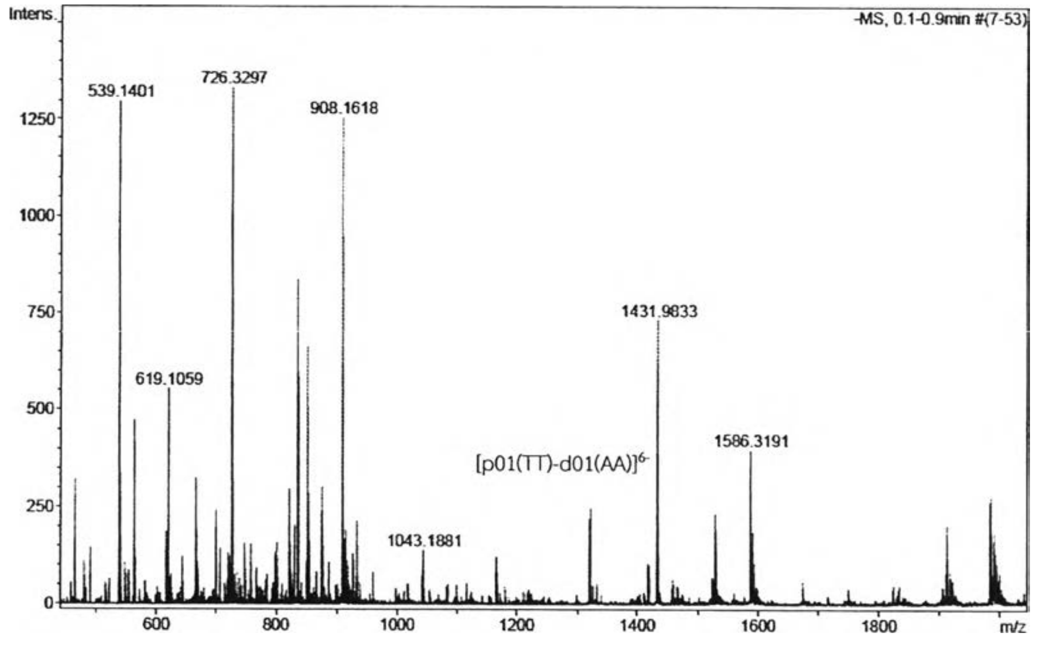

Figure A.20 Spectrum of duplex p01 (TT) - d01 (AA) at 22 eV.

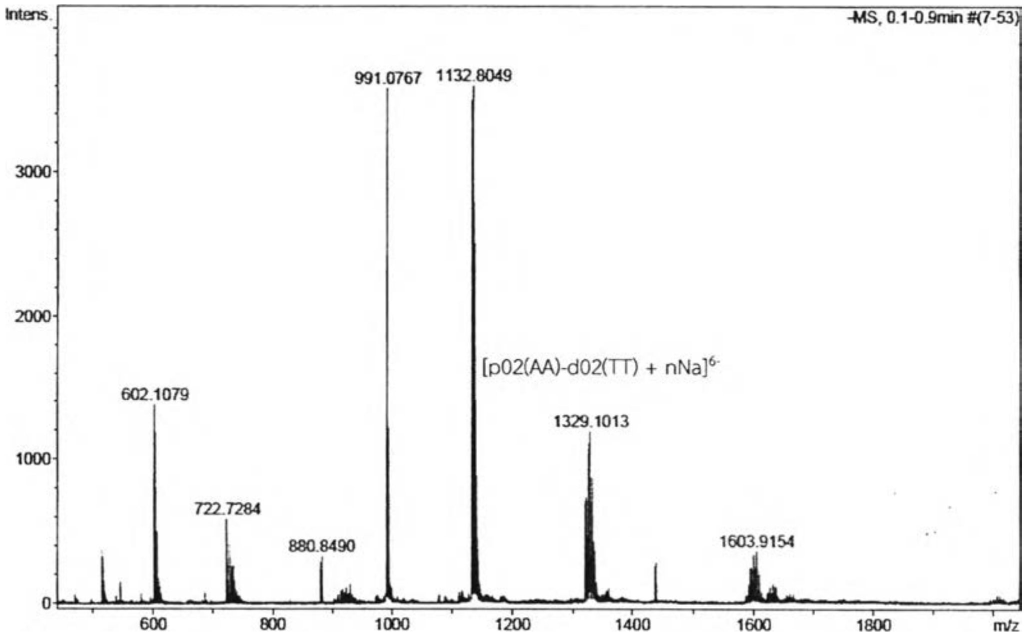

Figure A.45 Spectrum of duplex p02 (AA) - d02 (TT) at 0 eV.

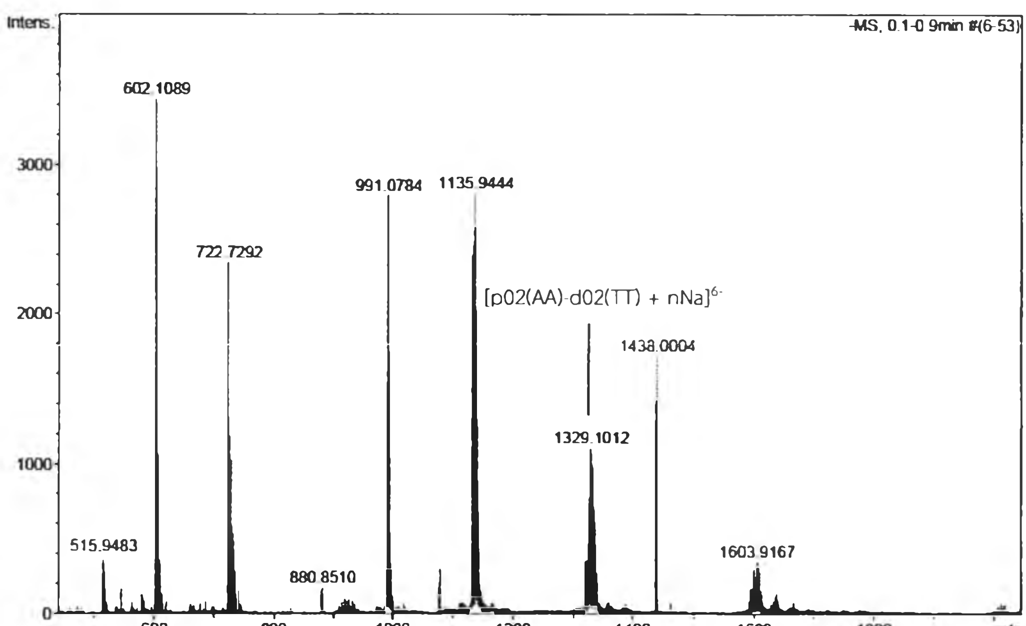

Figure A.46 Spectrum of duplex p02 (AA) - d02 (TT) at 2 eV.

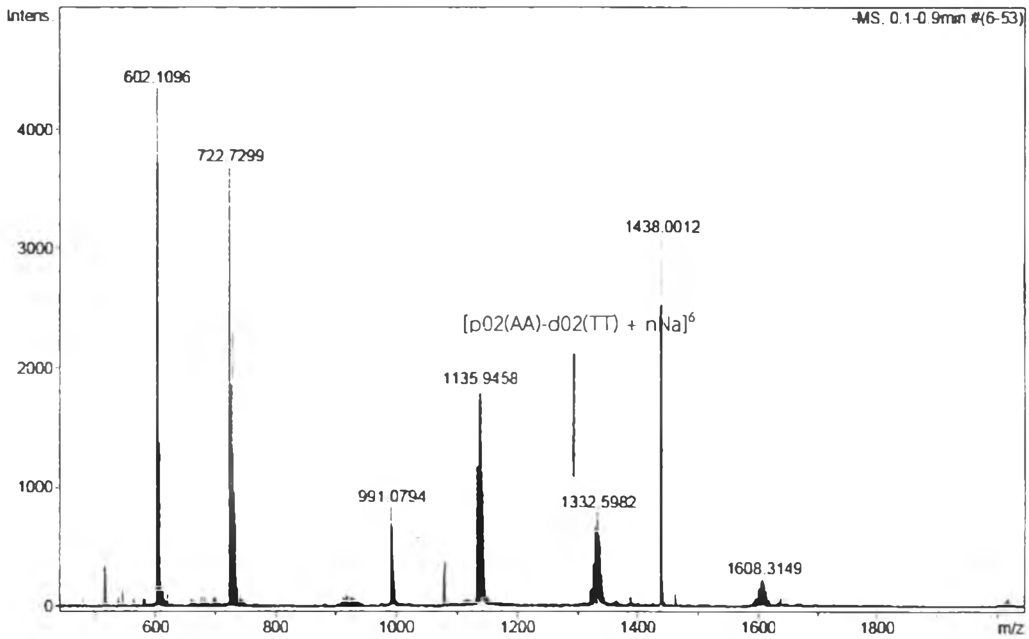

Figure A.47 Spectrum of duplex p02 (AA) - d02 (TT) at 4 eV.

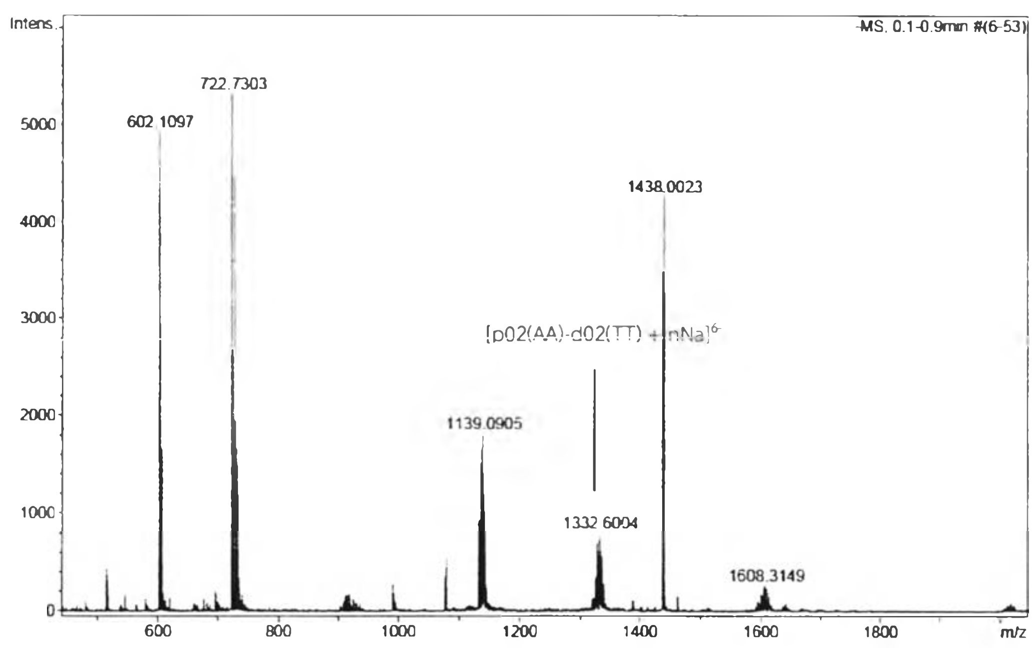

Figure A.48 Spectrum of duplex p02 (AA) - d02 (TT) at 6 eV.

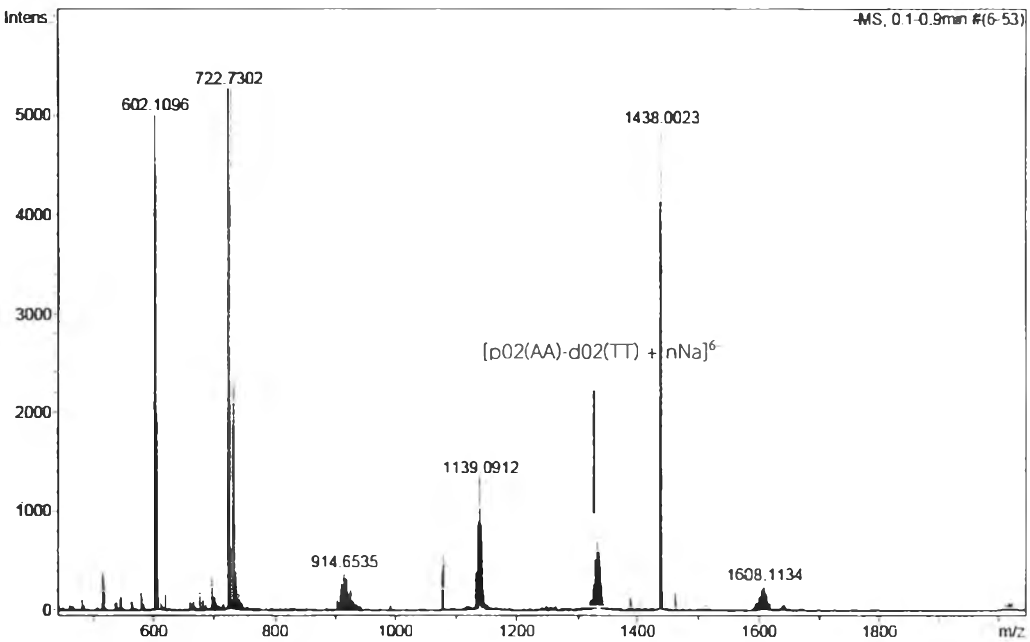

Figure A.49 Spectrum of duplex p02 (AA) - d02 (TT) at 8 eV.

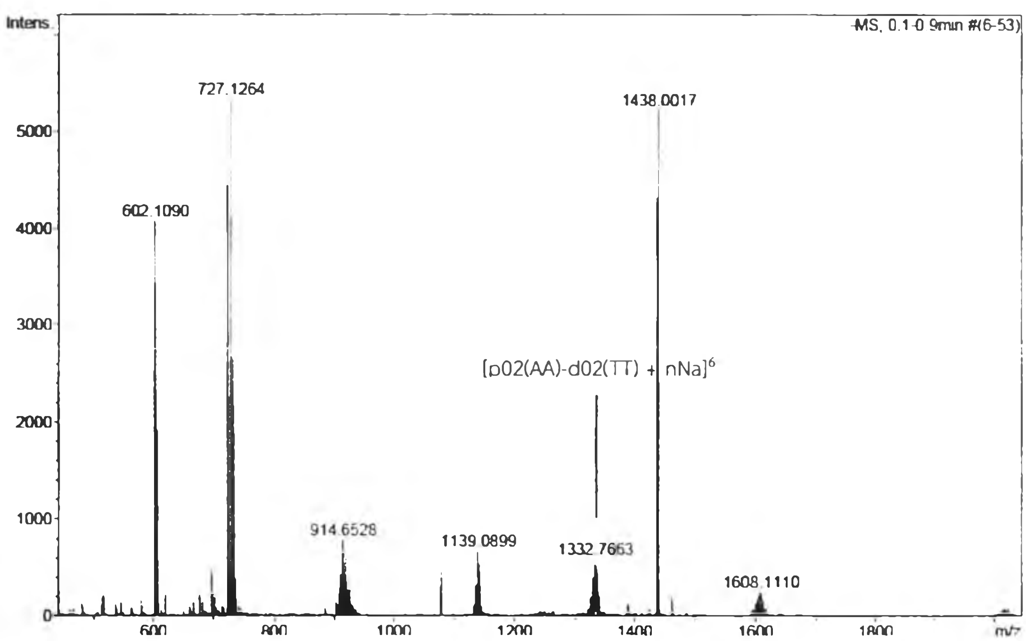

Figure A.50 Spectrum of duplex p02 (AA) - d02 (TT) at 10 eV.

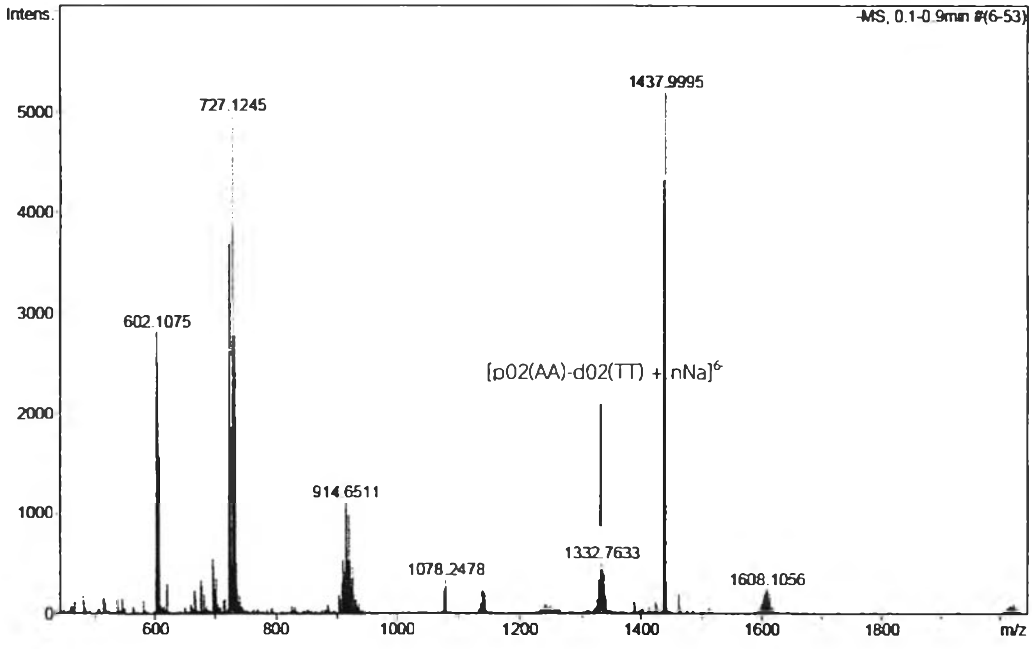

Figure A.51 Spectrum of duplex p02 (AA) - d02 (TT) at 12 eV.

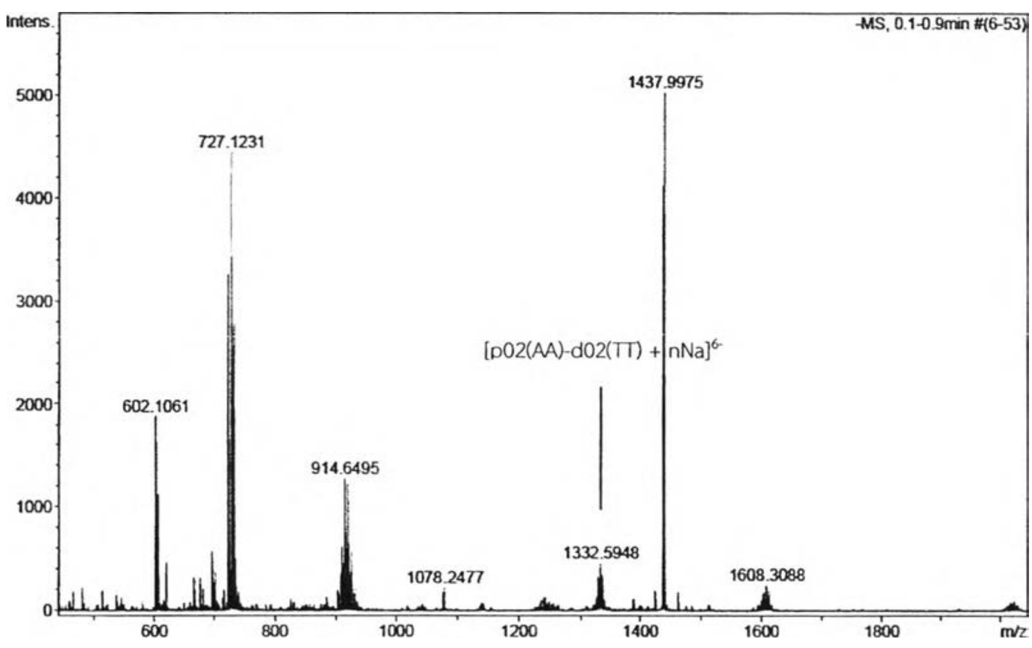

Figure A.52 Spectrum of duplex p02 (AA) - d02 (TT) at 14 eV.

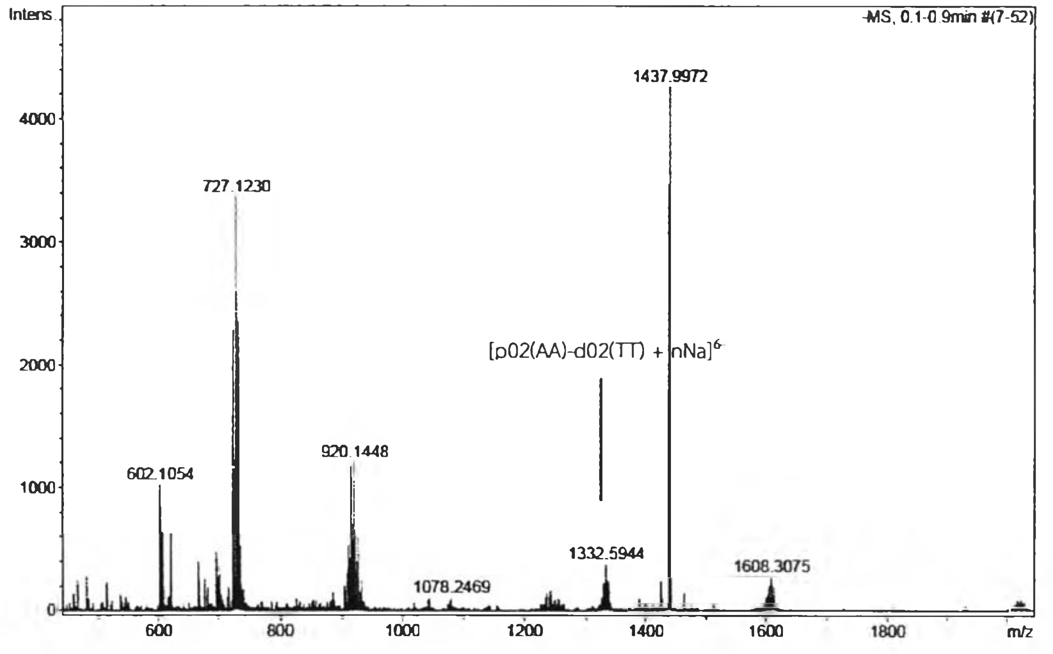

Figure A.53 Spectrum of duplex p02 (AA) - d02 (TT) at 16 eV.

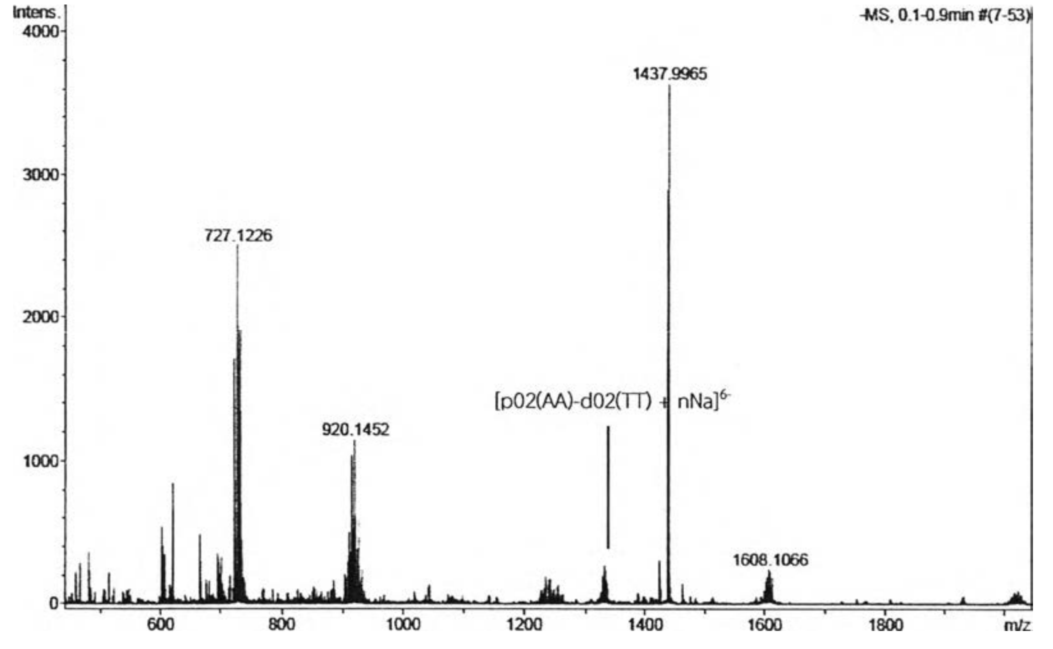

Figure A.54 Spectrum of duplex p02 (AA) - d02 (TT) at 18 eV.

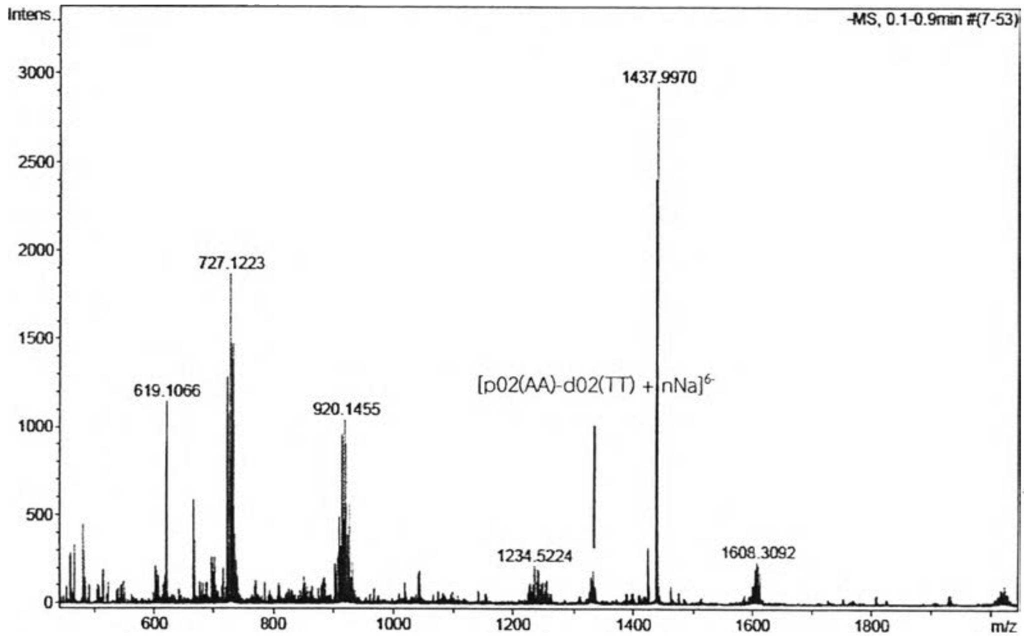

Figure A.55 Spectrum of duplex p02 (AA) - d02 (TT) at 20 eV.

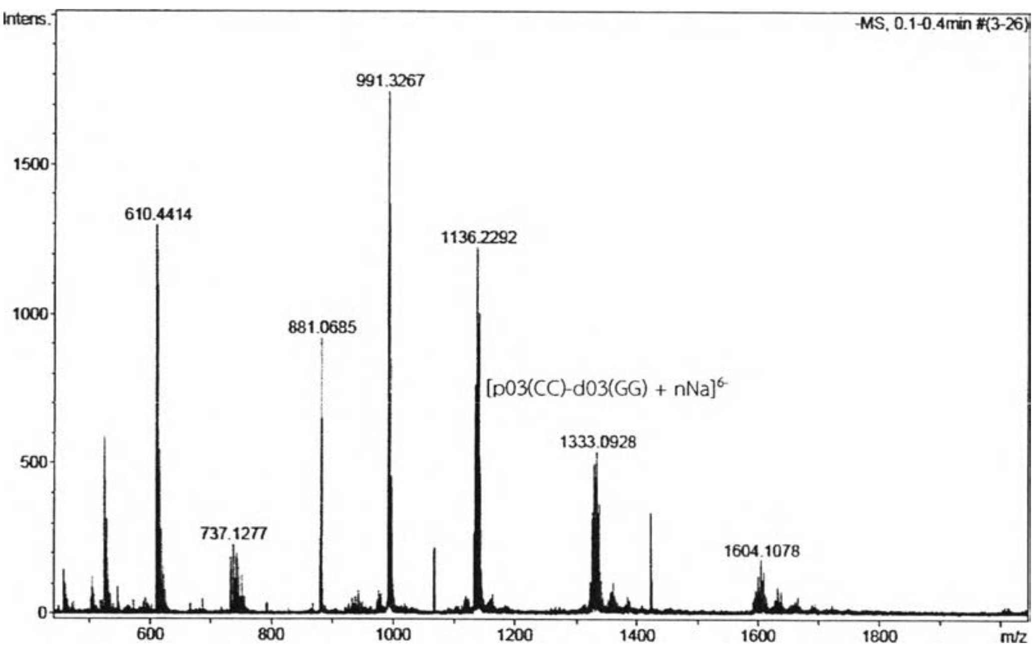

Figure A.78 Spectrum of duplex p03 (CC) - d03 (GG) at 0 eV.

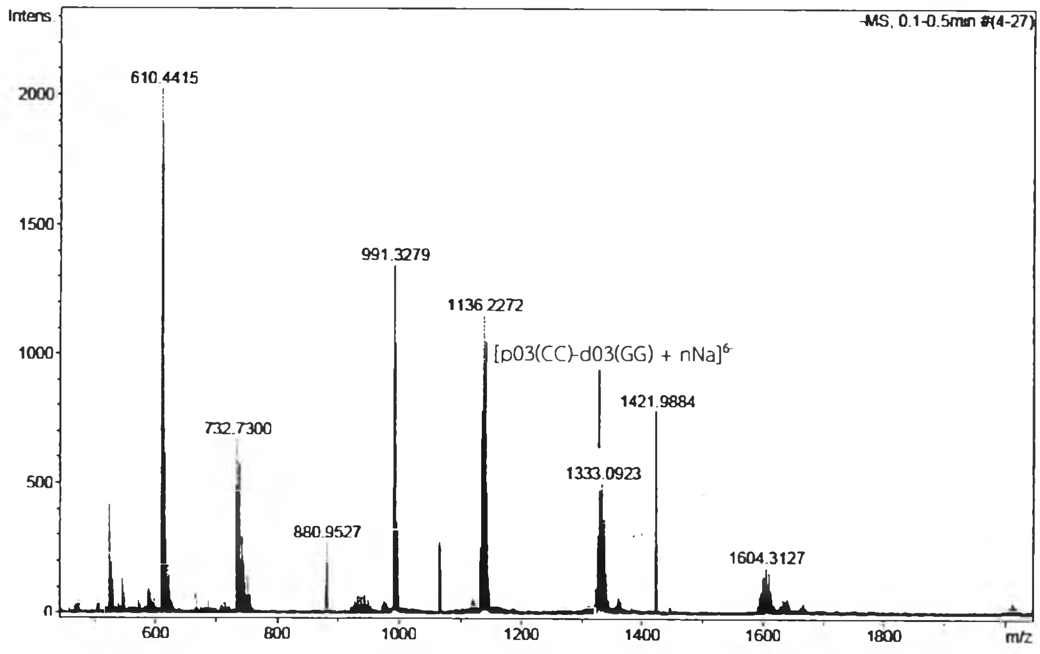

Figure A.79 Spectrum of duplex p03 (CC) - d03 (GG) at 2 eV.

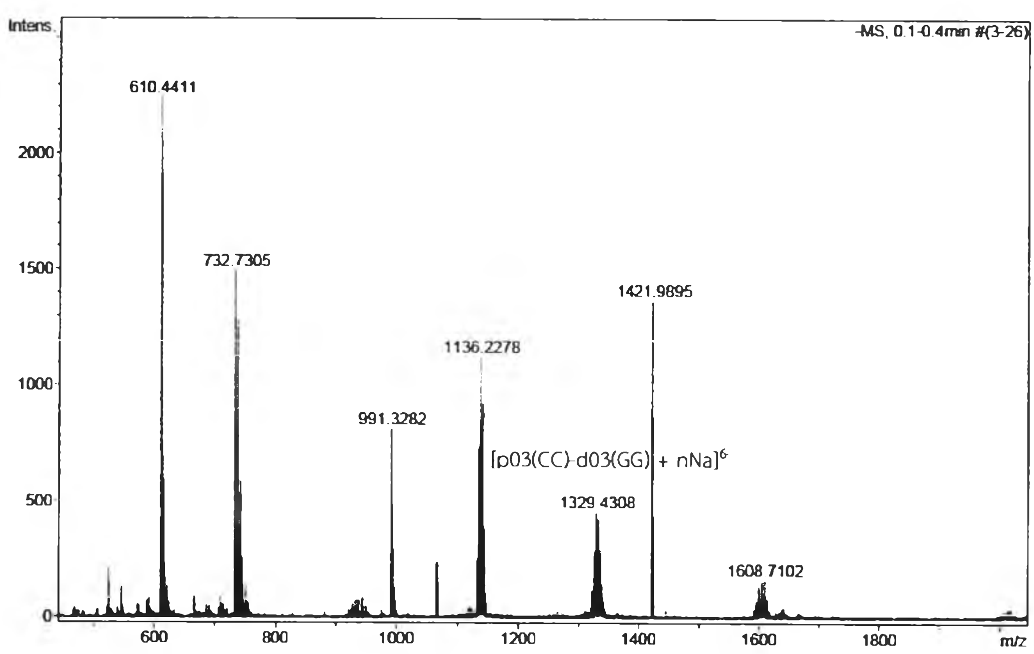

Figure A.80 Spectrum of duplex p03 (CC) - d03 (GG) at 4 eV.

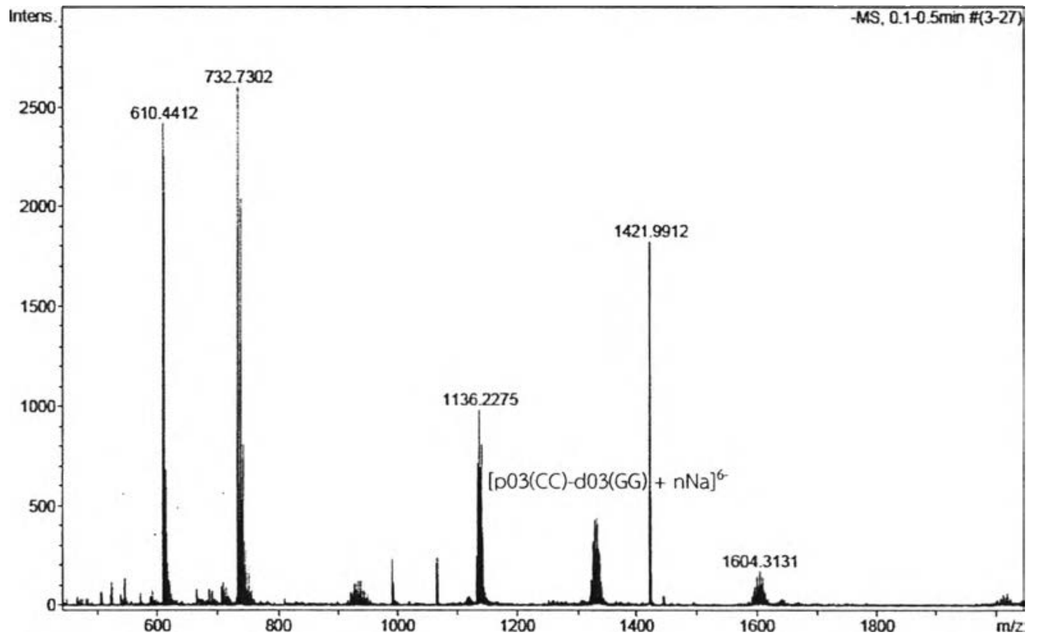

Figure A.81 Spectrum of duplex p03 (CC) - d03 (GG) at 6 eV.

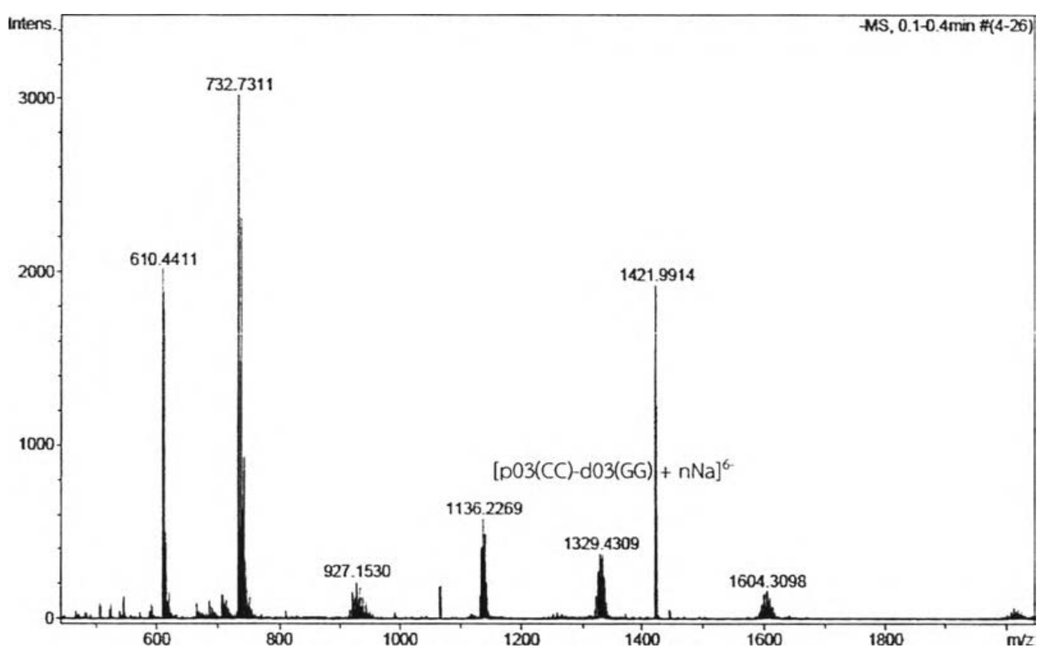

Figure A.82 Spectrum of duplex p03 (CC) - d03 (GG) at 8 eV.

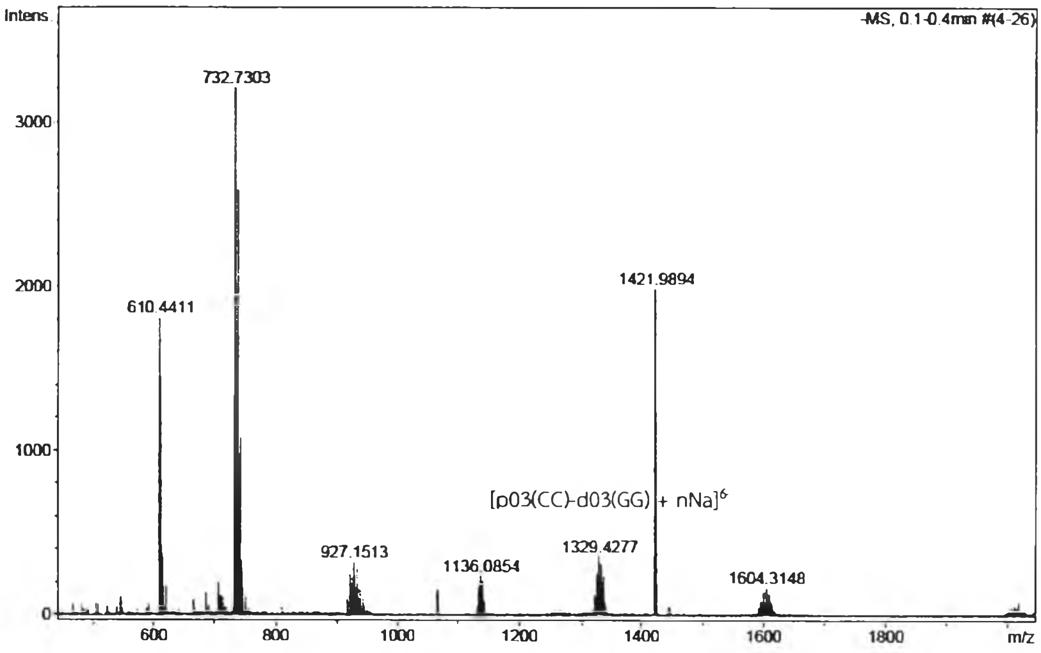

Figure A.83 Spectrum of duplex p03 (CC) - d03 (GG) at 10 eV.

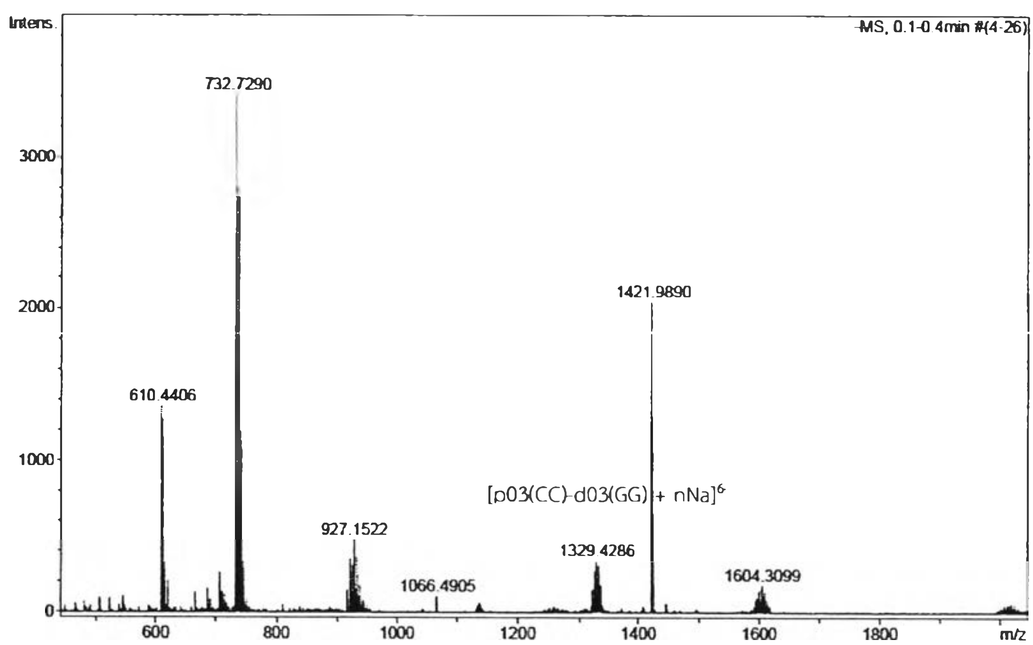

Figure A.84 Spectrum of duplex p03 (CC) - d03 (GG) at 12 eV.

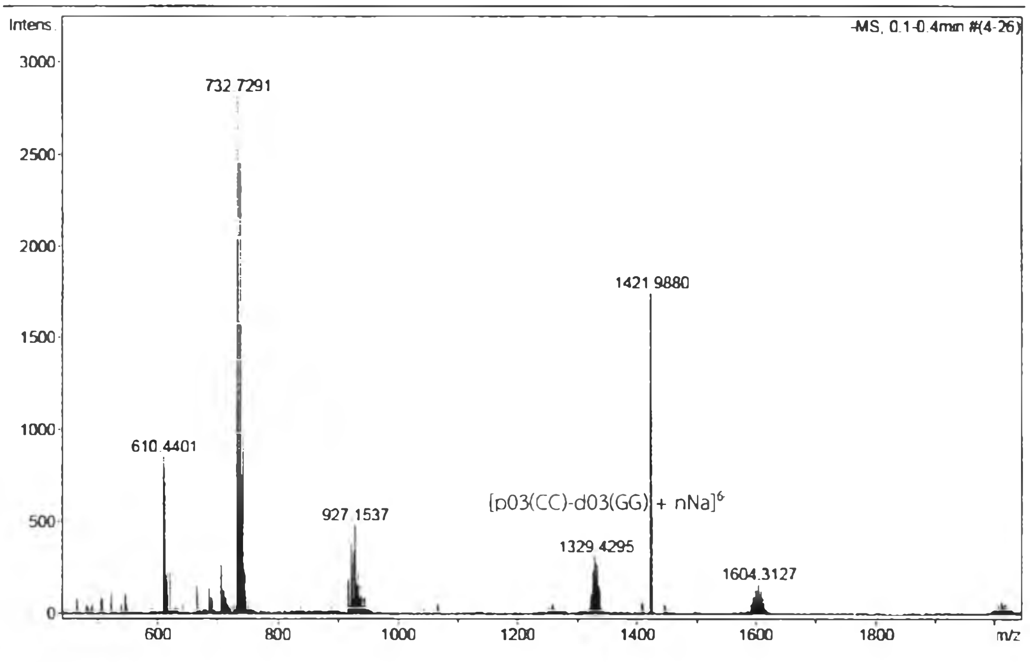

Figure A.85 Spectrum of duplex p03 (CC) - d03 (GG) at 14 eV.

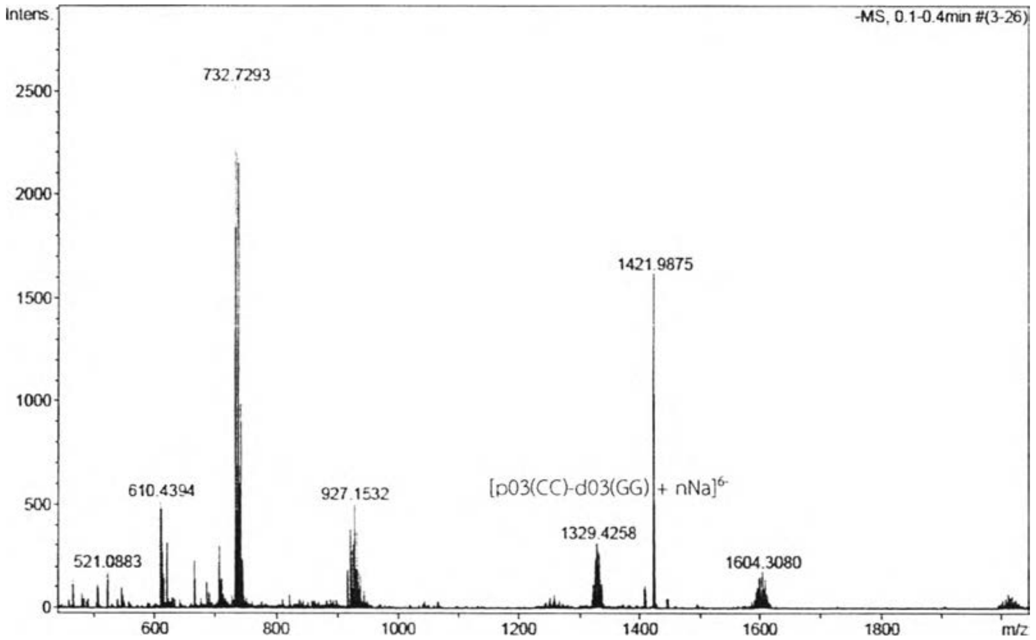

Figure A.86 Spectrum of duplex p03 (CC) - d03 (GG) at 16 eV.

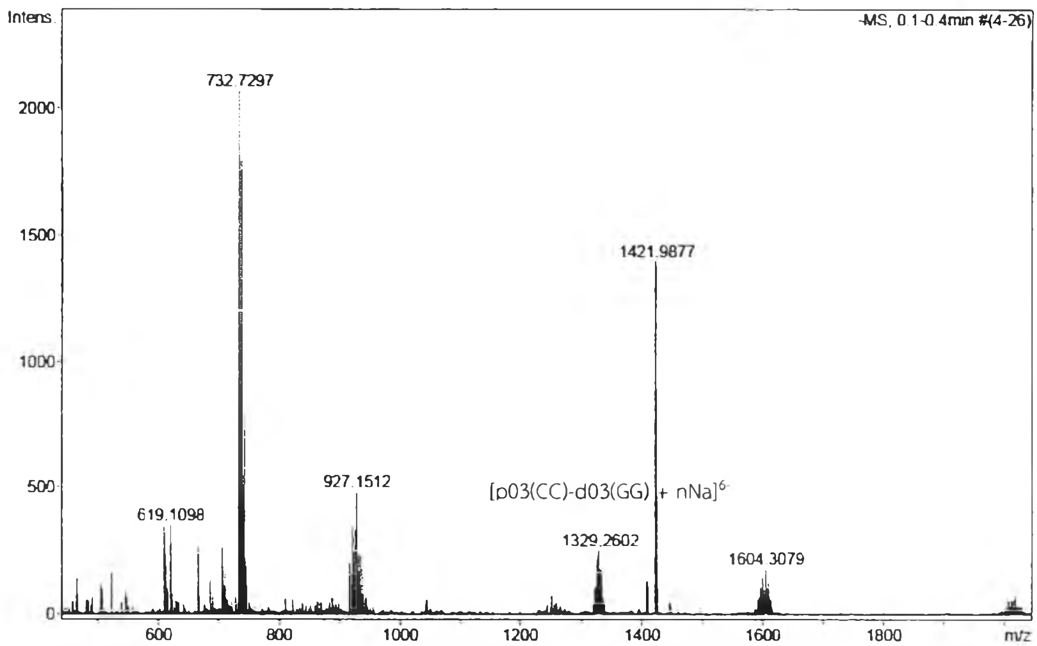

Figure A.87 Spectrum of duplex p03 (CC) - d03 (GG) at 18 eV.

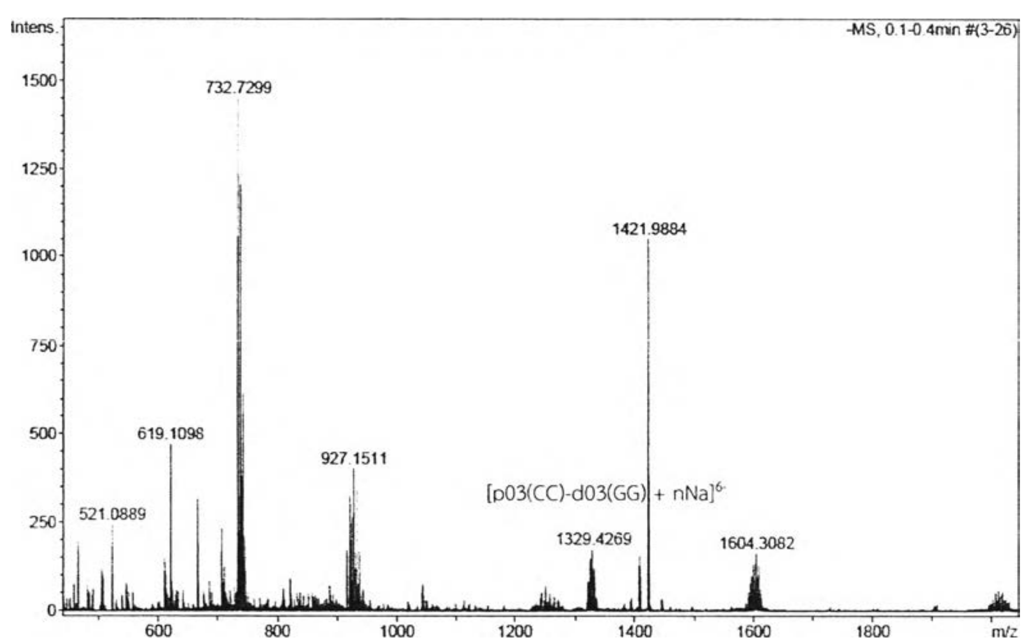

Figure A.88 Spectrum of duplex p03 (CC) - d03 (GG) at 20 eV.

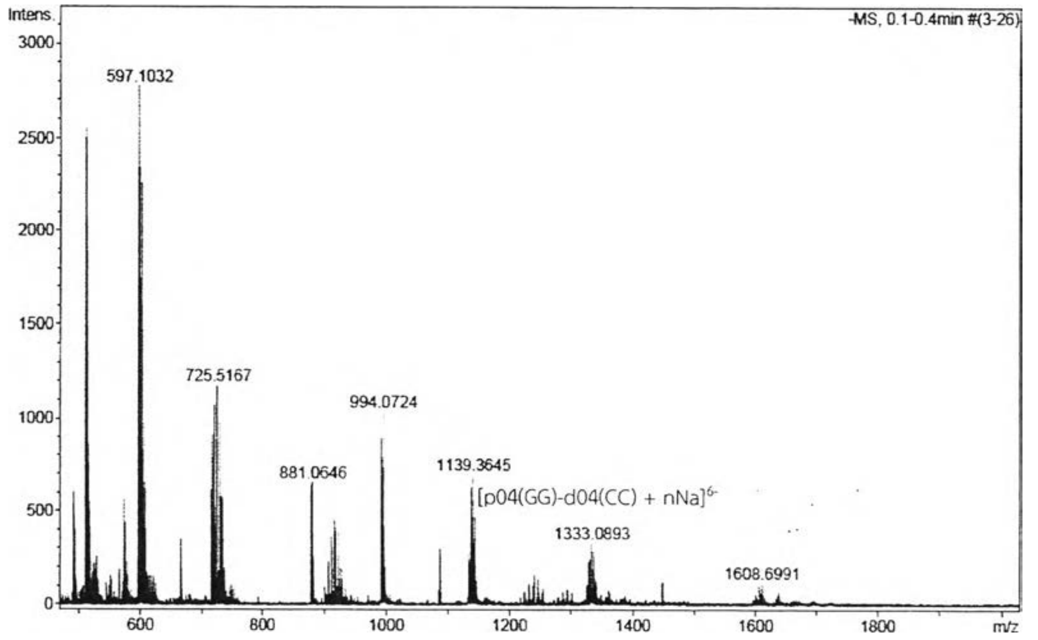

Figure A.111 Spectrum of duplex p04 (GG) - d04 (CC) at 0 eV.

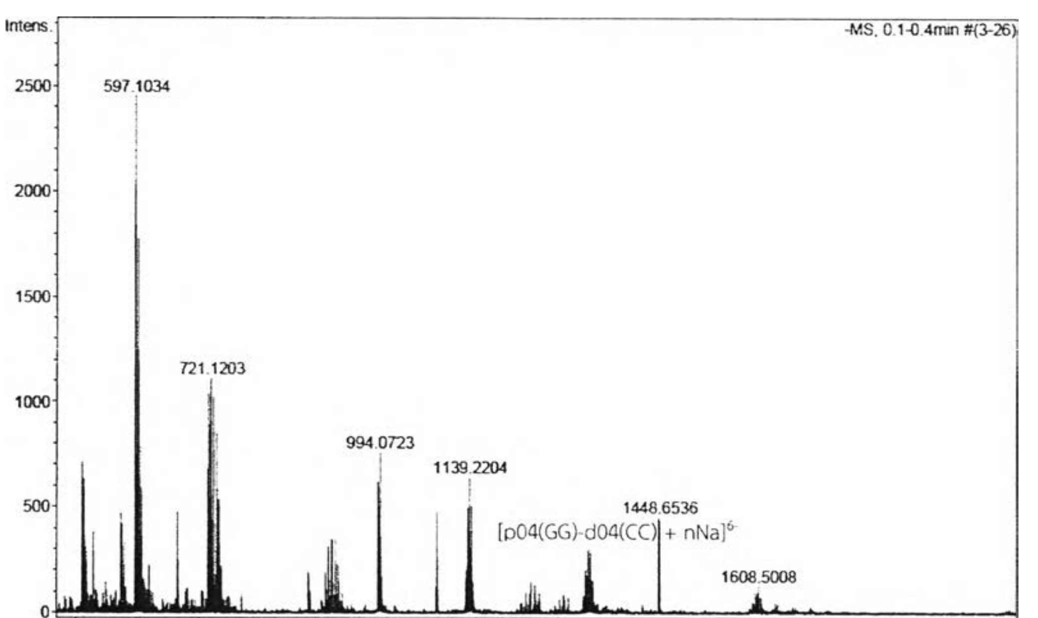

Figure A.112 Spectrum of duplex p04 (GG) - d04 (CC) at 2 eV.

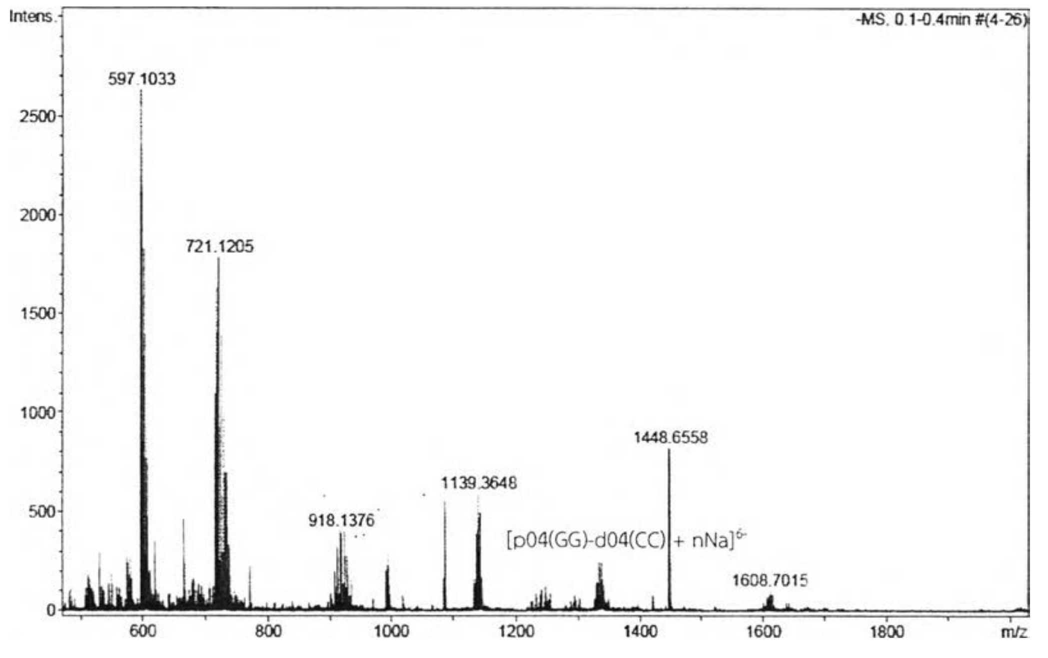

Figure A.113 Spectrum of duplex p04 (GG) - d04 (CC) at 4 eV.

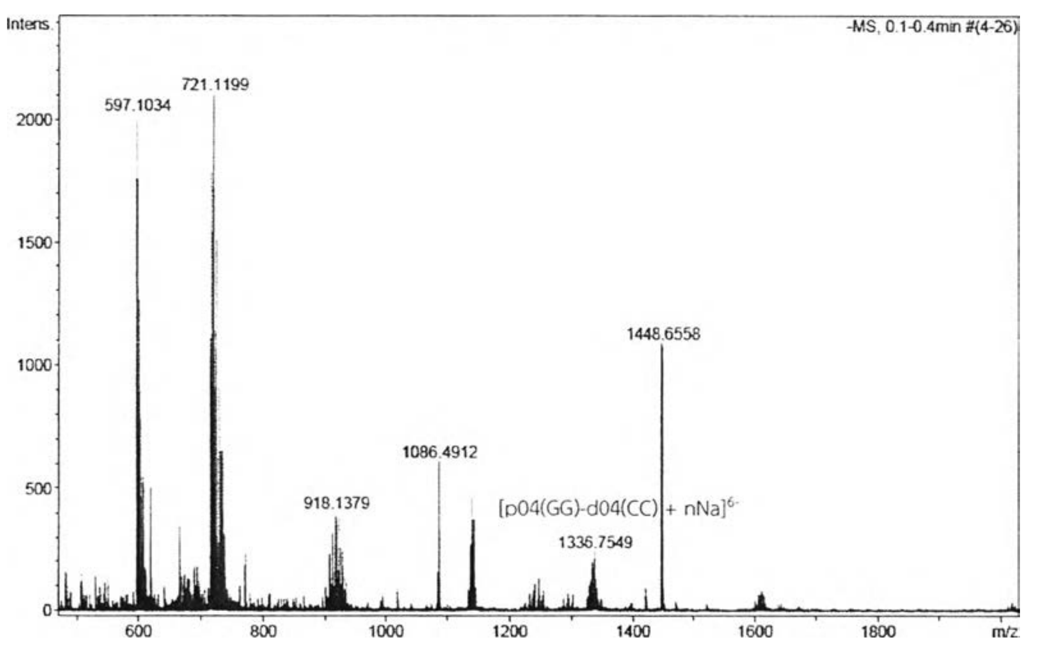

Figure A.114 Spectrum of duplex p04 (GG) - d04 (CC) at 6 eV.

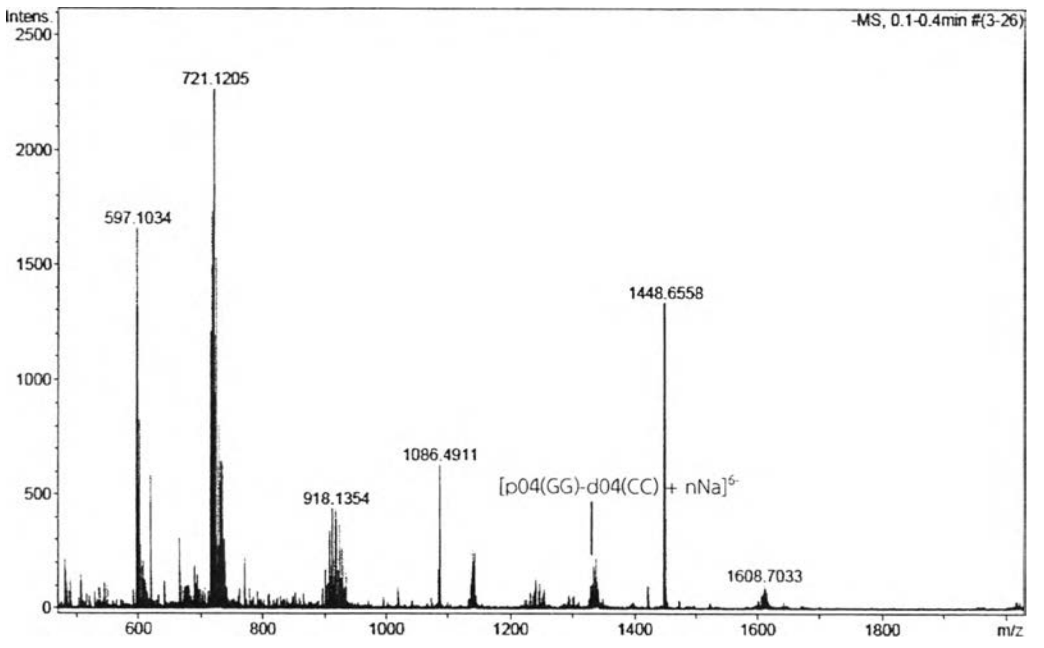

Figure A.115 Spectrum of duplex p04 (GG) - d04 (CC) at 8 eV.

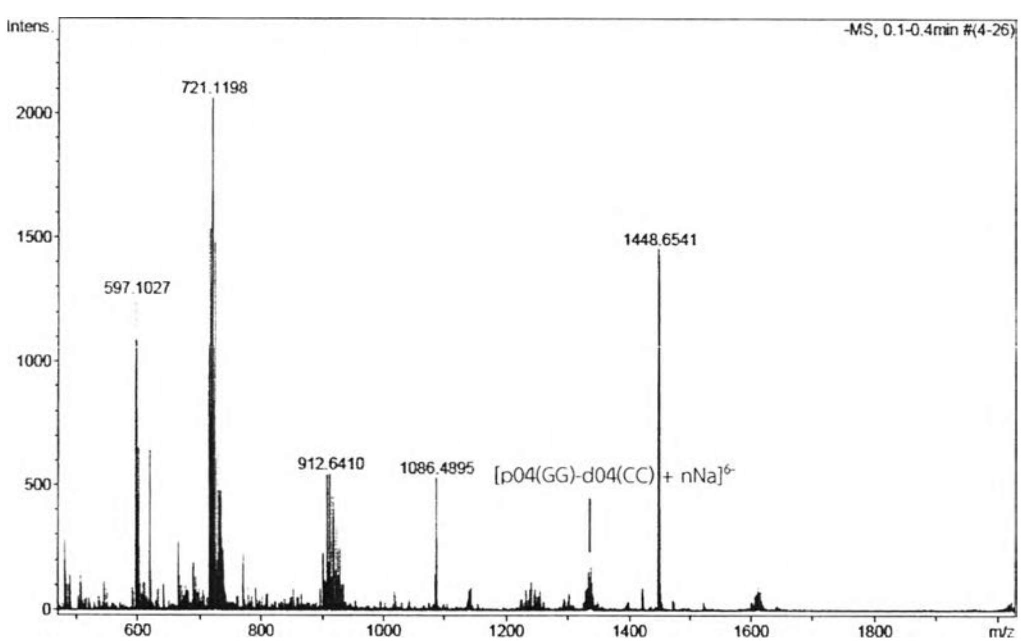

Figure A.116 Spectrum of duplex p04 (GG) - d04 (CC) at 10 eV.

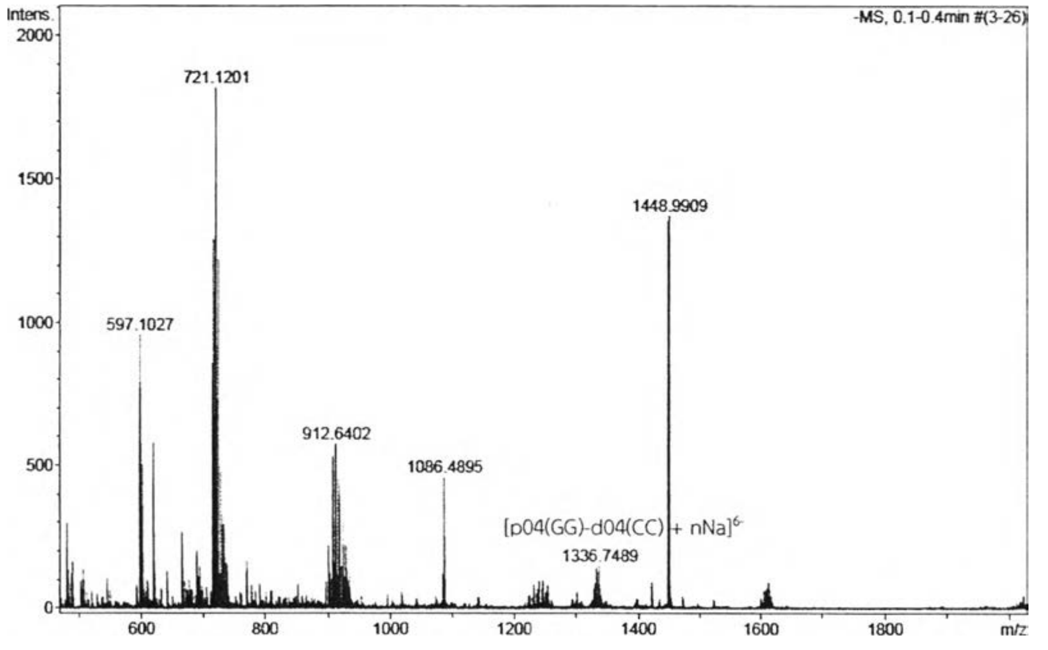

Figure A.117 Spectrum of duplex p04 (GG) - d04 (CC) at 12 eV.

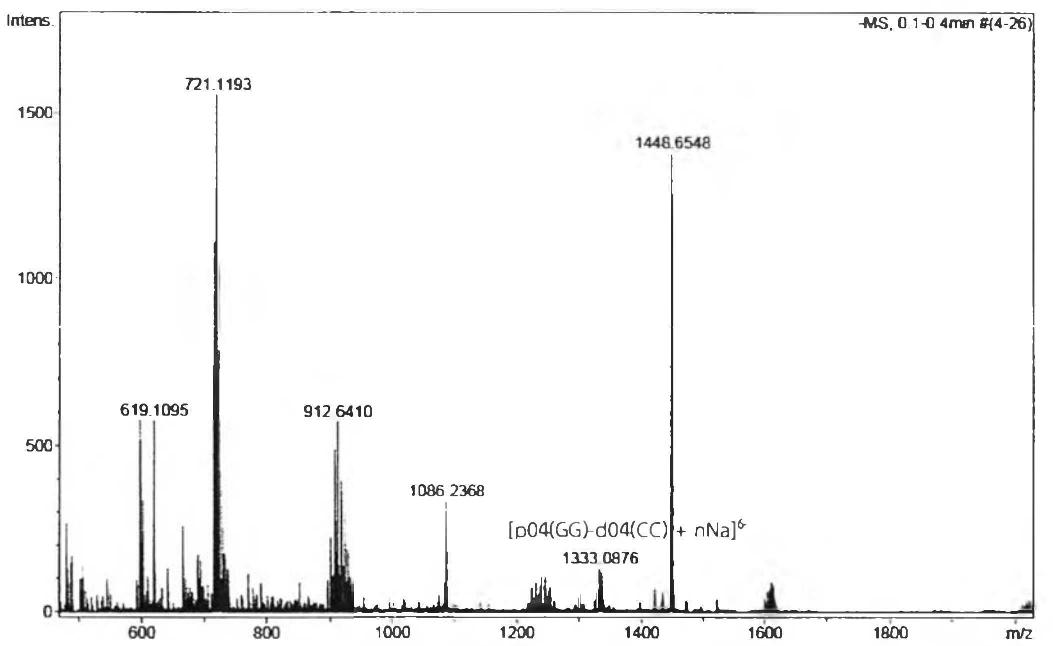

Figure A.118 Spectrum of duplex p04 (GG) - d04 (CC) at 14 eV.

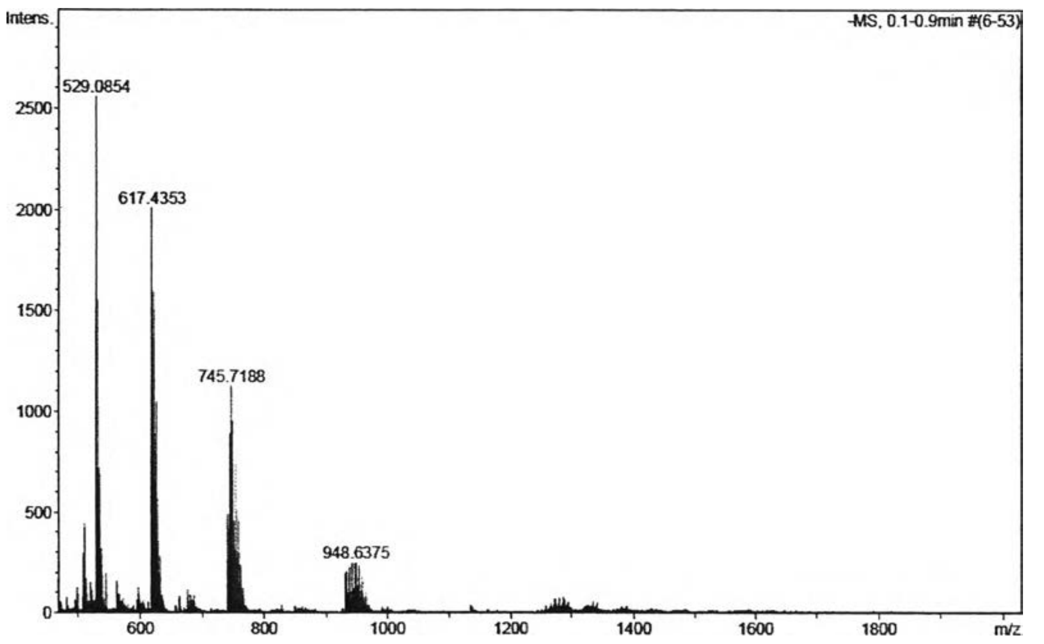

Figure A.135 Spectrum of duplex p05 - d05 at 0 eV.

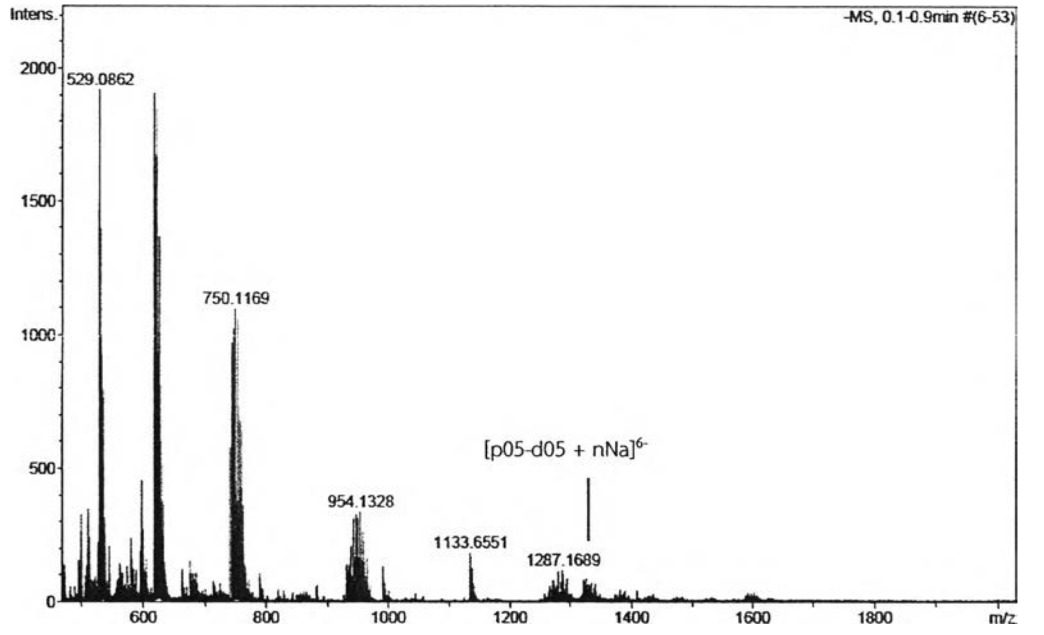

Figure A.136 Spectrum of duplex p05 - d05 at 2 eV.

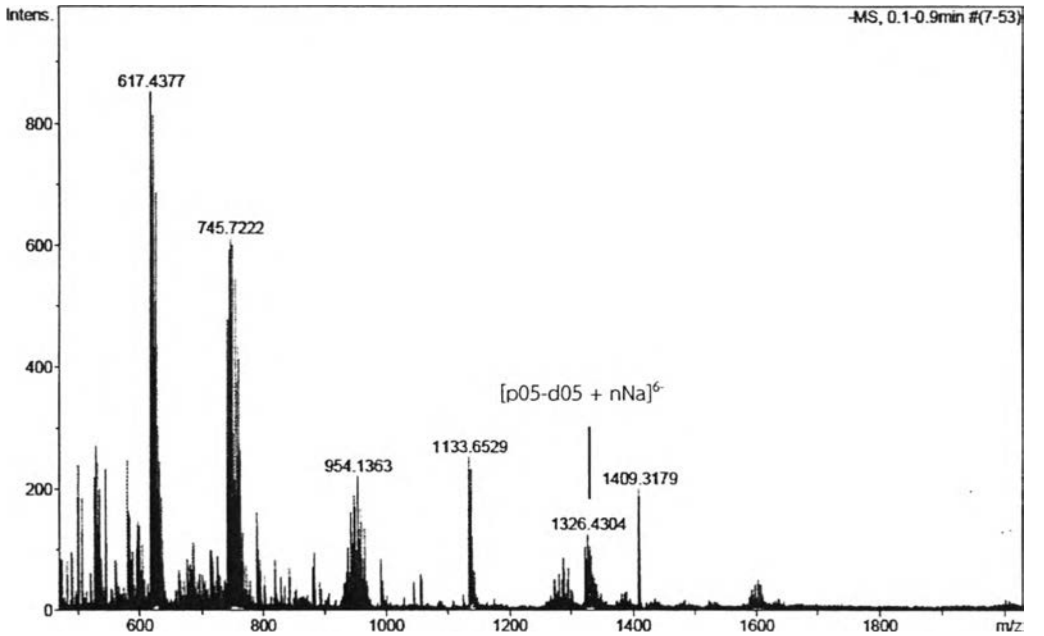

Figure A.137 Spectrum of duplex p05 - d05 at 4 eV.

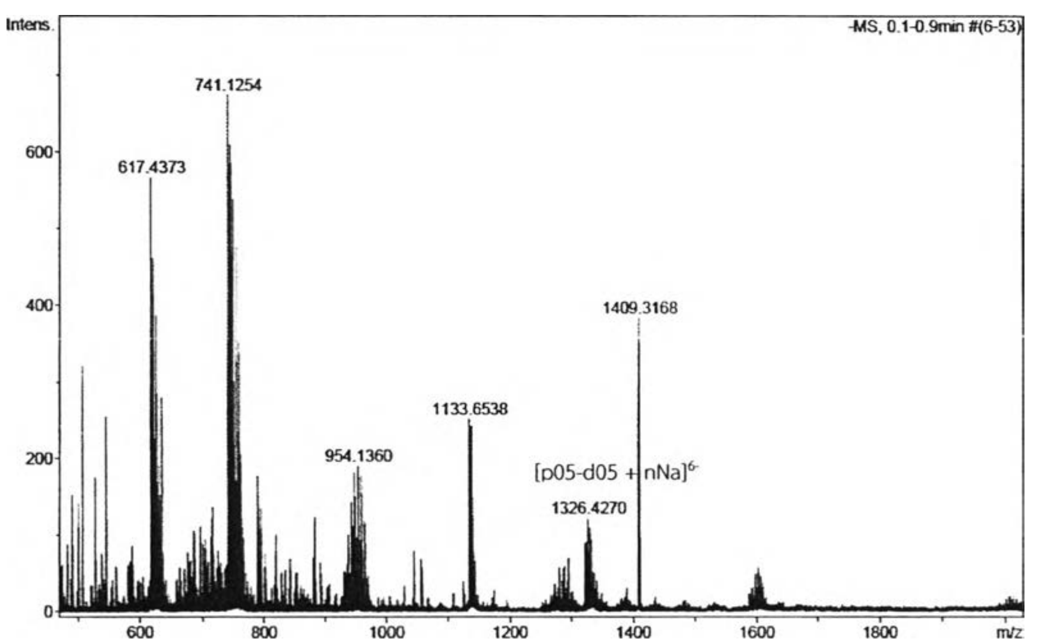

Figure A.138 Spectrum of duplex p05 - d05 at 6 eV.

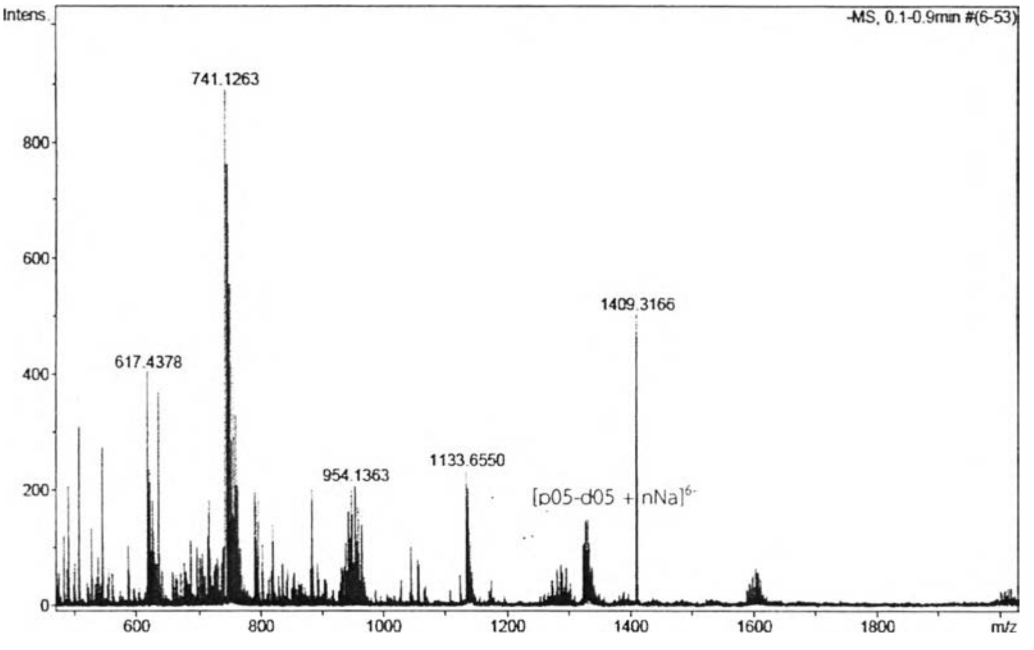

Figure A.139 Spectrum of duplex p05 - d05 at 8 eV.

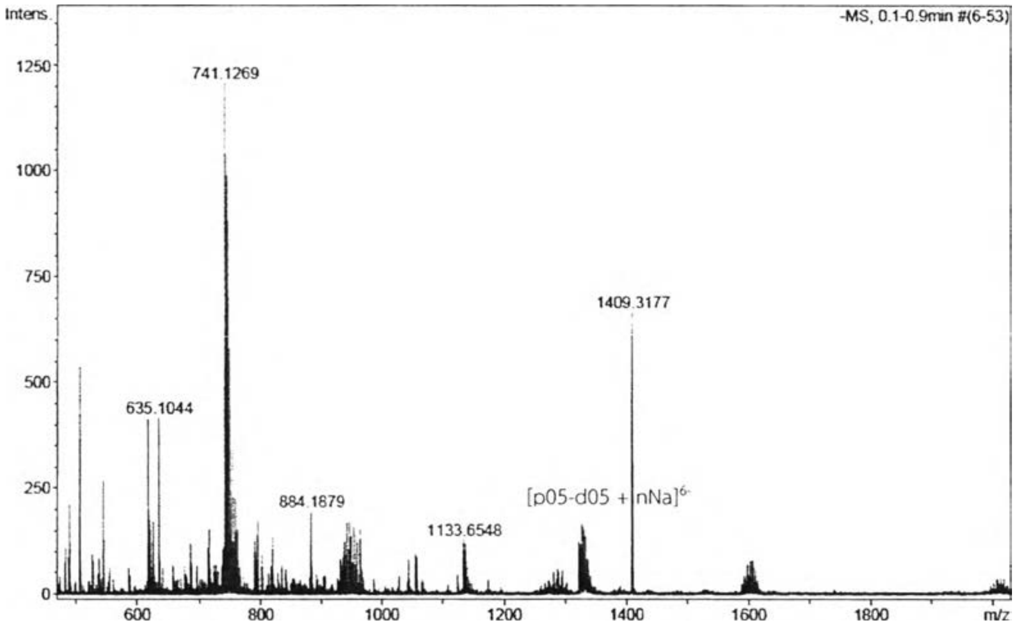

Figure A.140 Spectrum of duplex p05 - d05 at 10 eV.

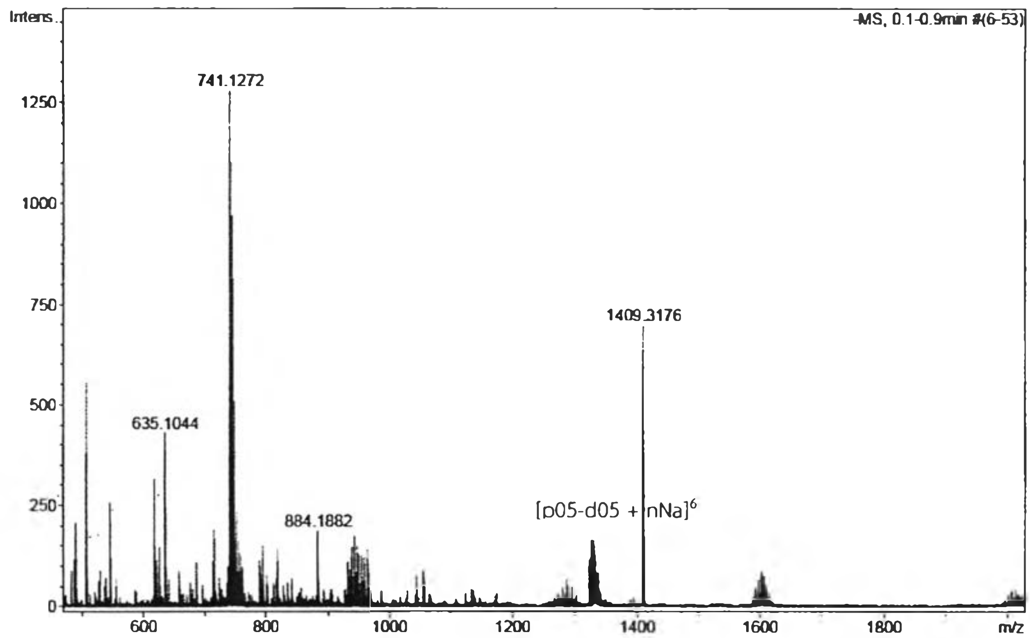

Figure A.141 Spectrum of duplex p05 - d05 at 12 eV.

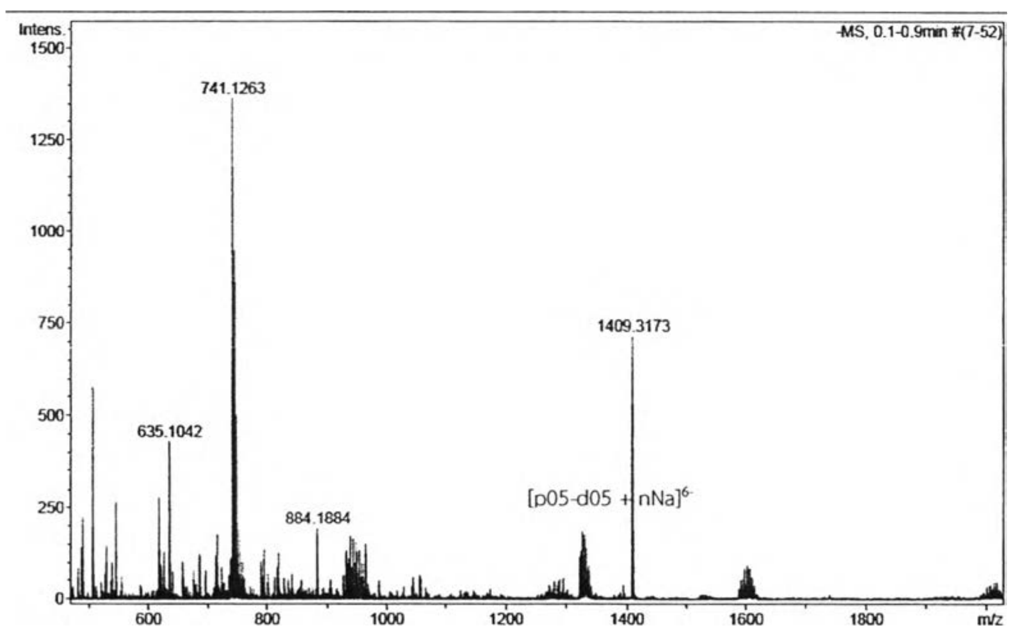

Figure A.142 Spectrum of duplex p05 - d05 at 14 eV.

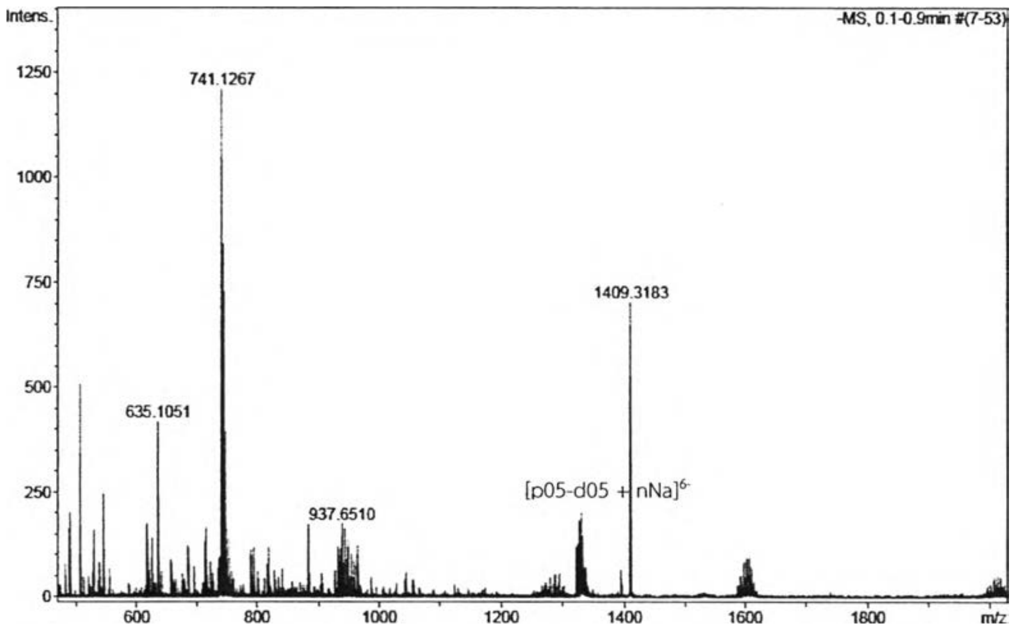

Figure A.143 Spectrum of duplex p05 - d05 at 16 eV.

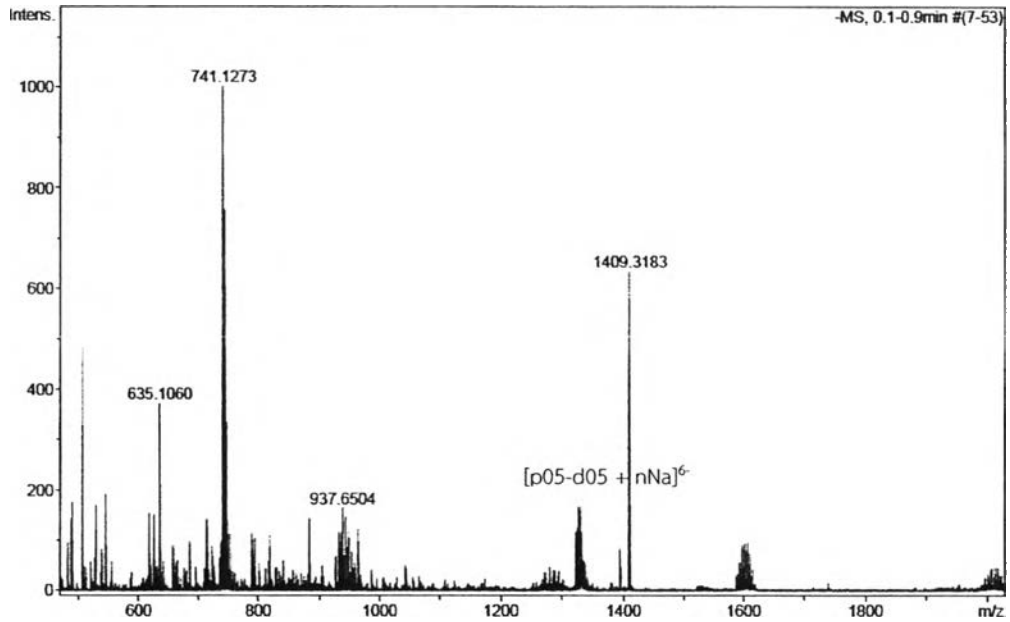

Figure A.144 Spectrum of duplex p05 - d05 at 18 eV.

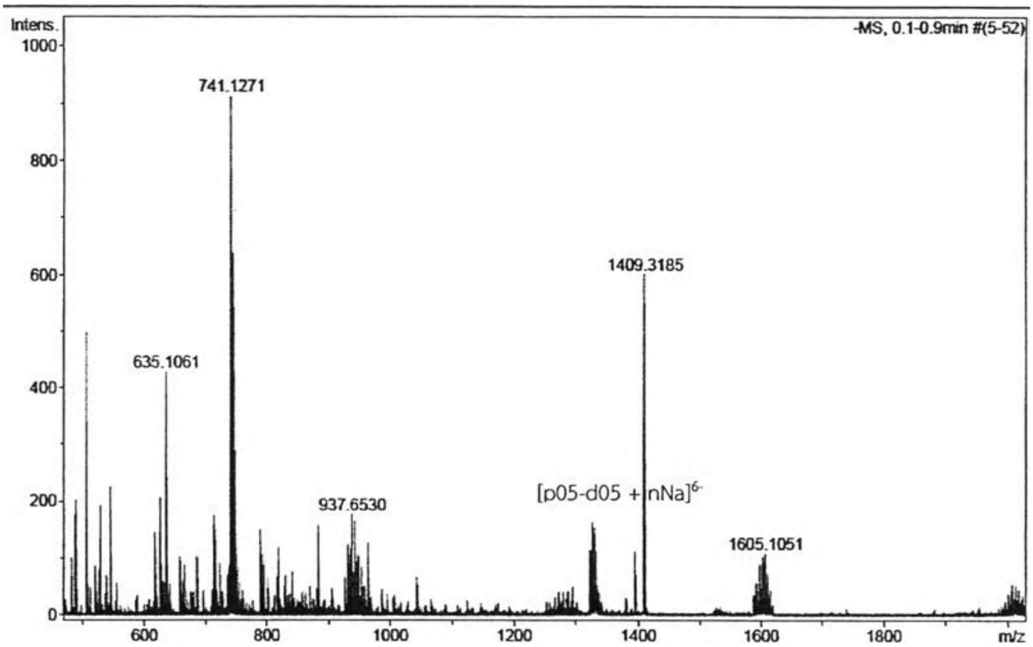

Figure A.145 Spectrum of duplex p05 - d05 at 20 eV.

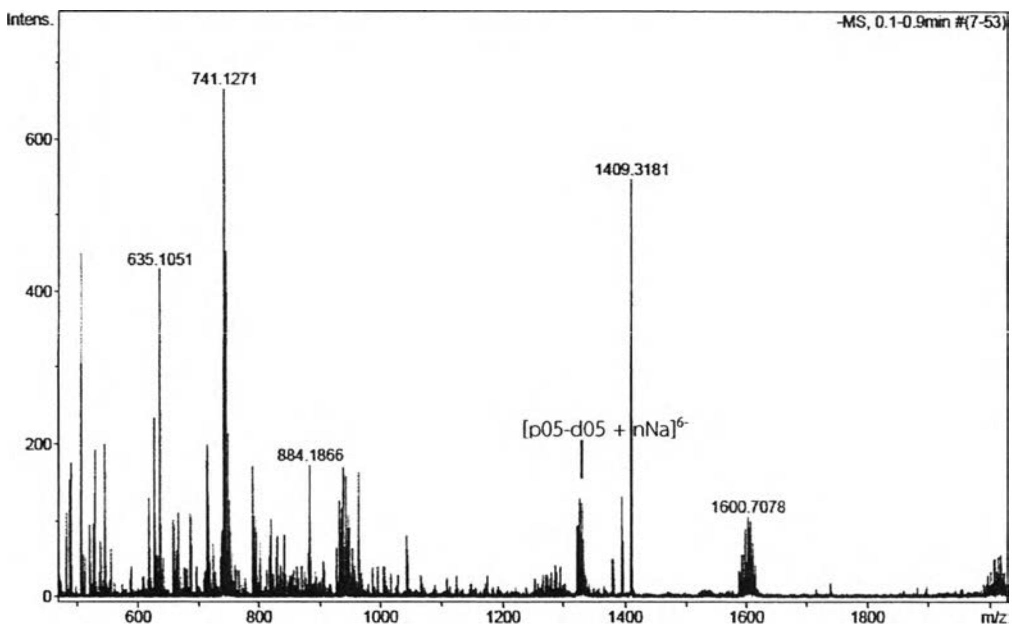

Figure A.146 Spectrum of duplex p05 - d05 at 22 eV.

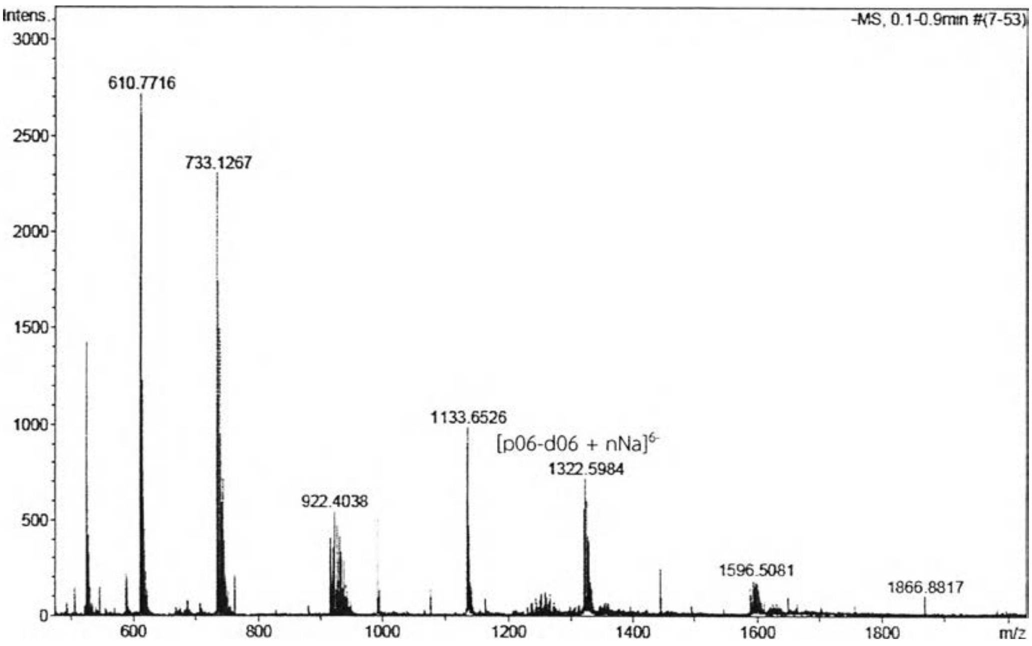

Figure A.180 Spectrum of duplex p06 - d06 at 0 eV.

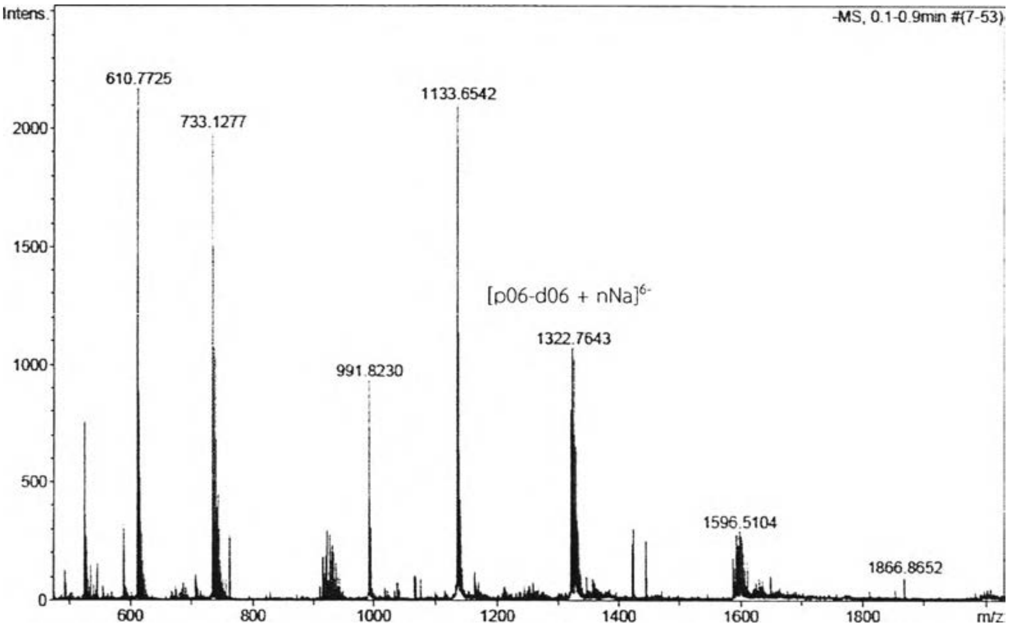

Figure A.181 Spectrum of duplex p06 - d06 at 2 eV.

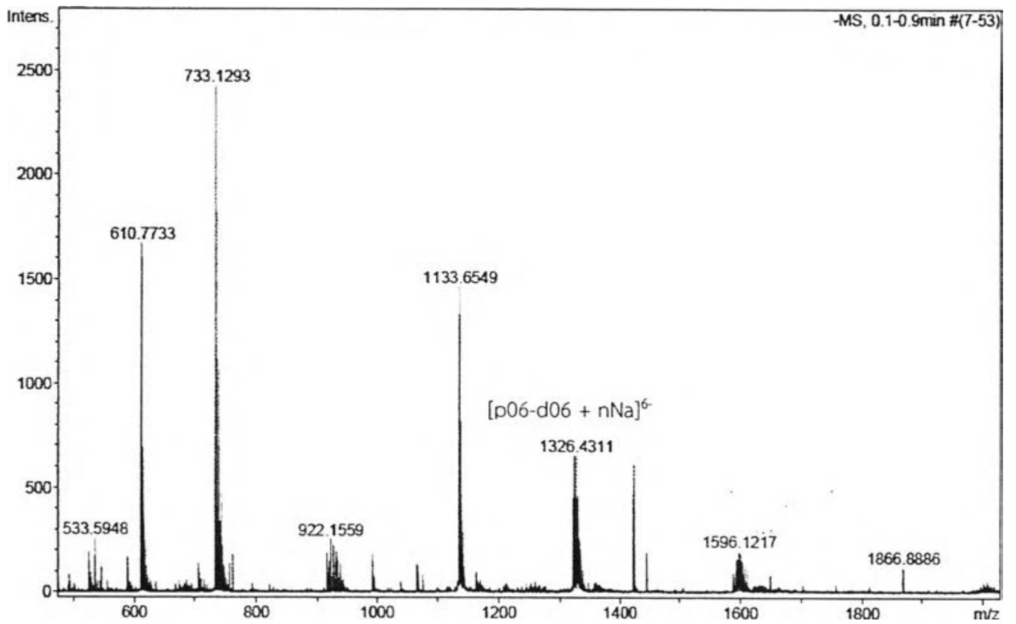

Figure A.182 Spectrum of duplex p06 - d06 at 4 eV.

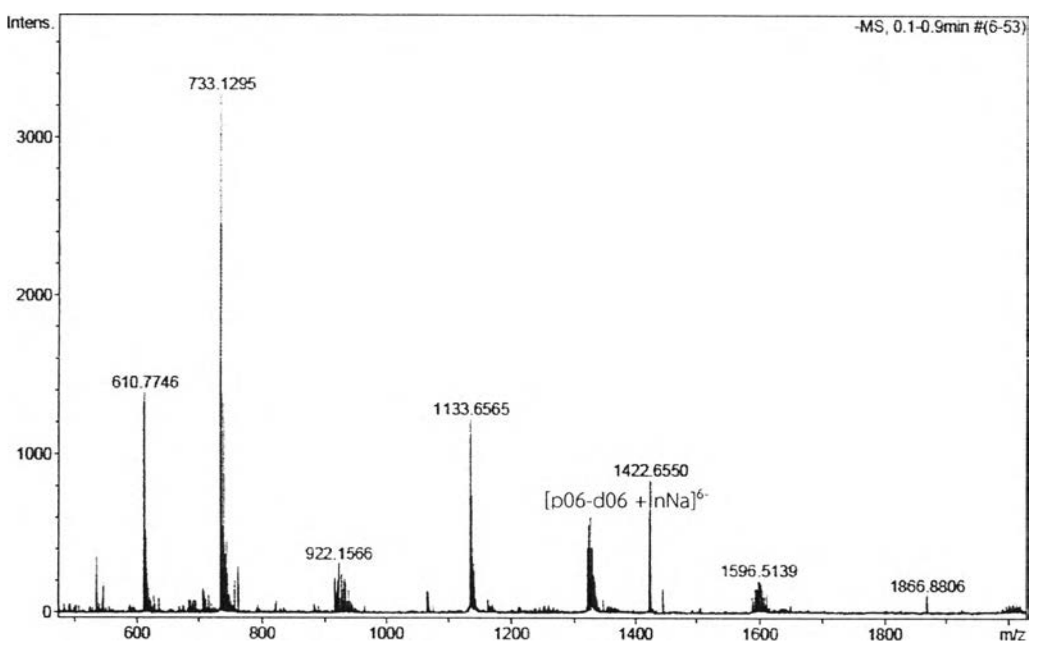

Figure A.183 Spectrum of duplex p06 - d06 at 6 eV.

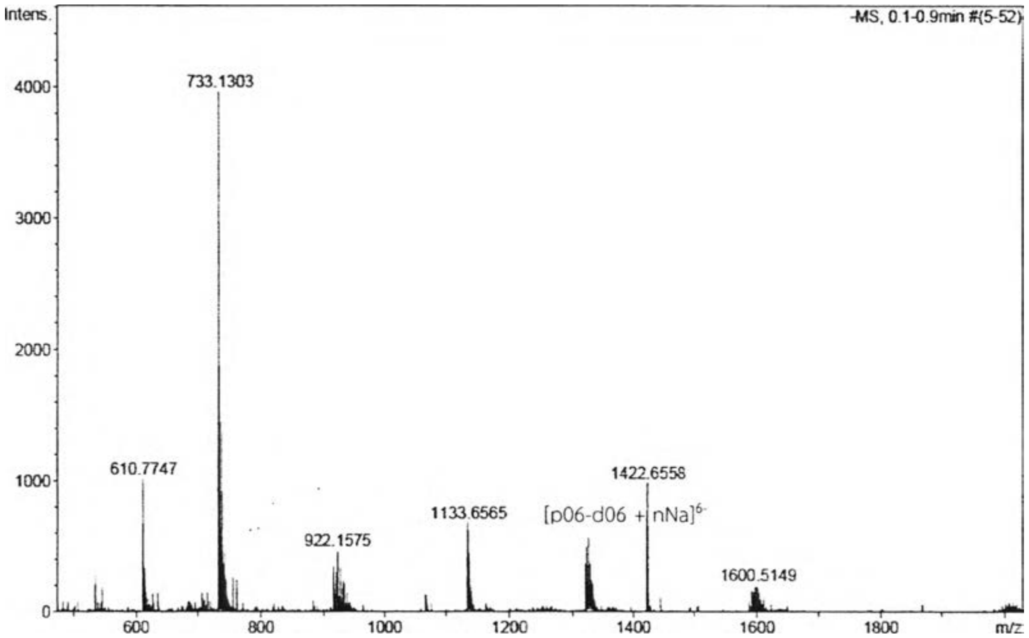

Figure A.184 Spectrum of duplex p06 - d06 at 8 eV.

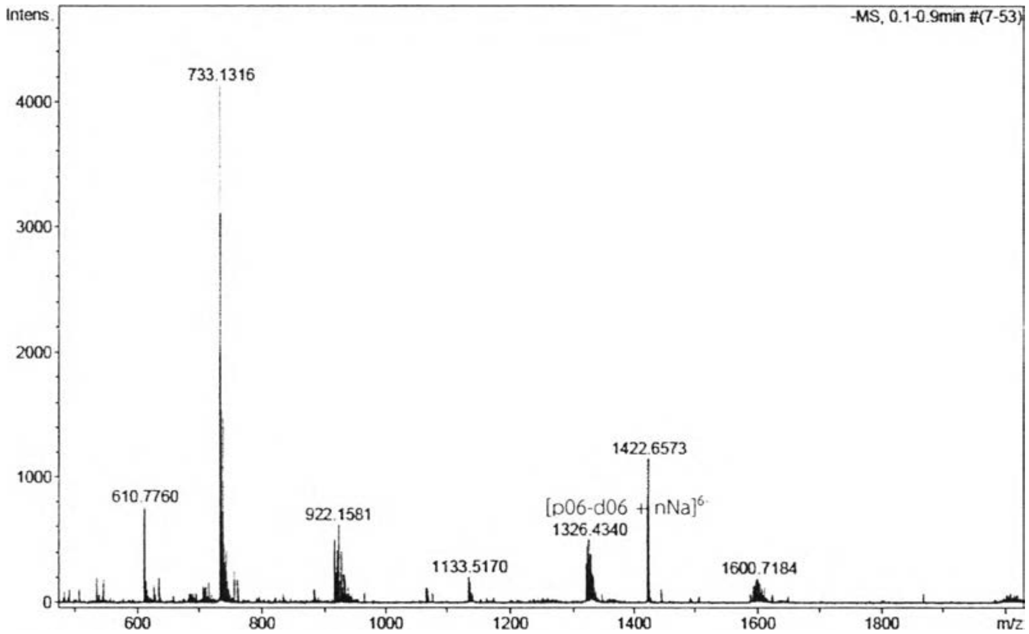

Figure A.185 Spectrum of duplex p06 - d06 at 10 eV.

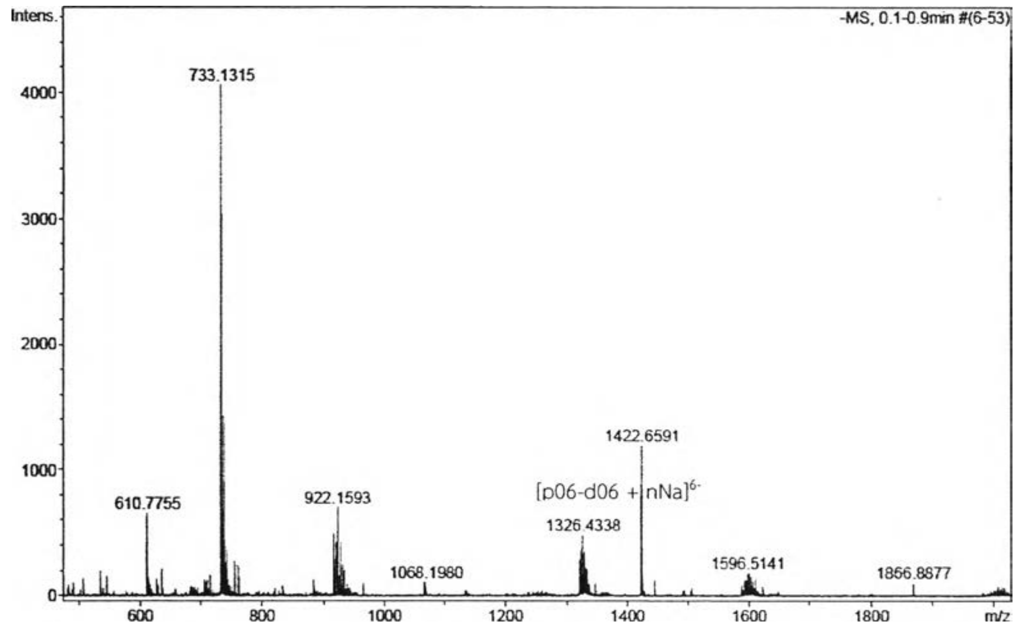

Figure A.186 Spectrum of duplex p06 - d06 at 12 eV.

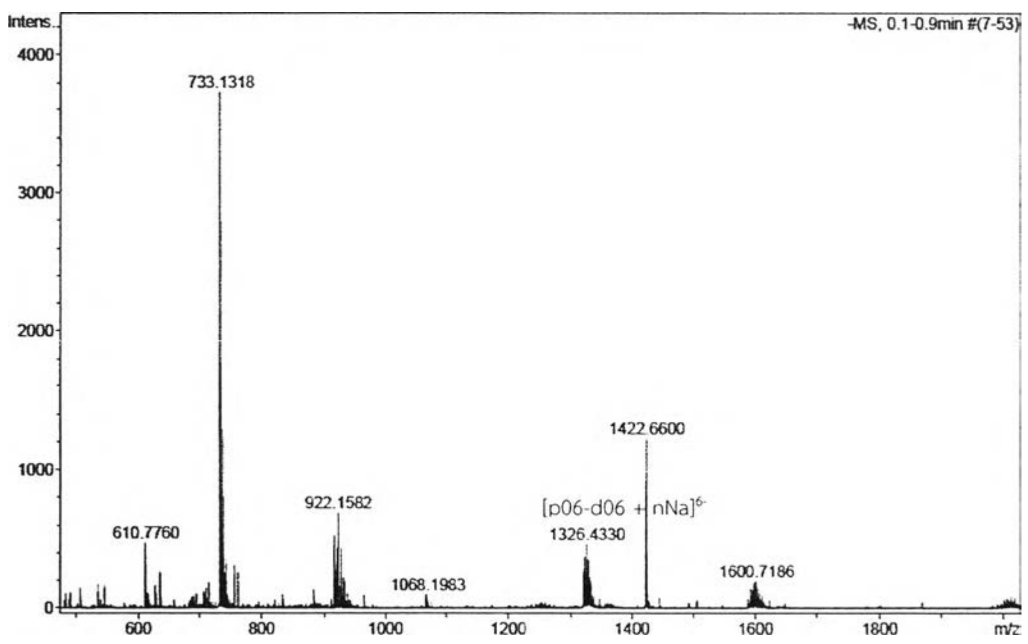

Figure A.187 Spectrum of duplex p06 - d06 at 14 eV.

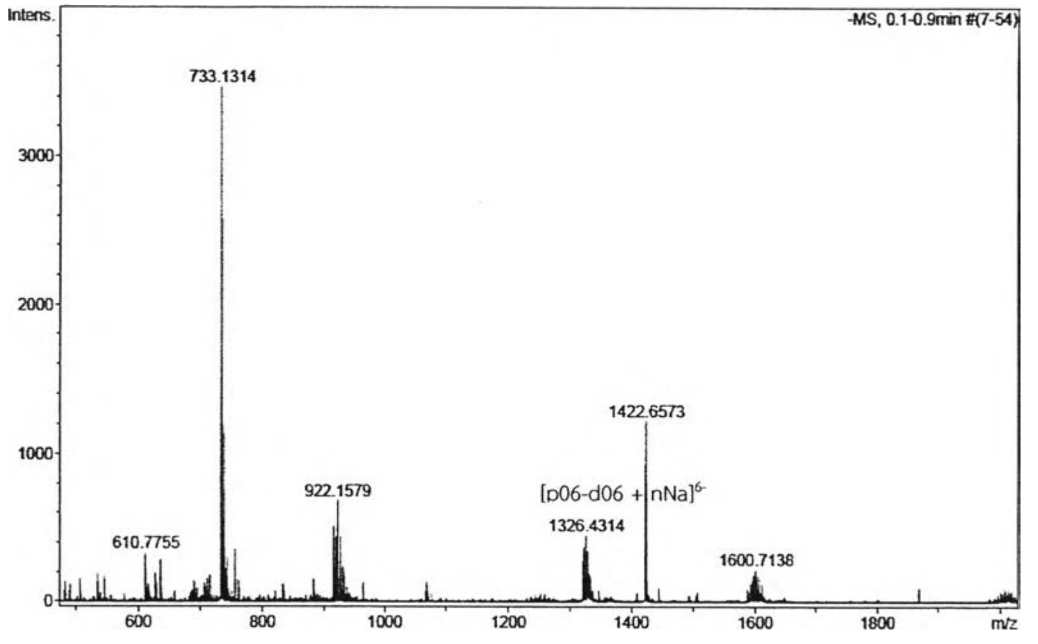

Figure A.188 Spectrum of duplex p06 - d06 at 16 eV.

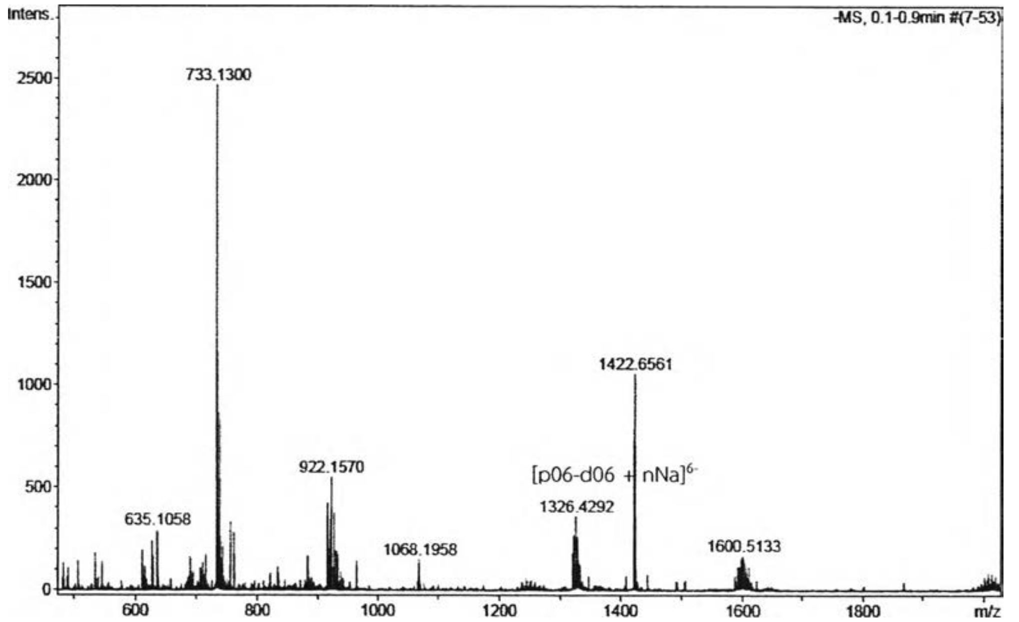

Figure A.189 Spectrum of duplex p06 - d06 at 18 eV.

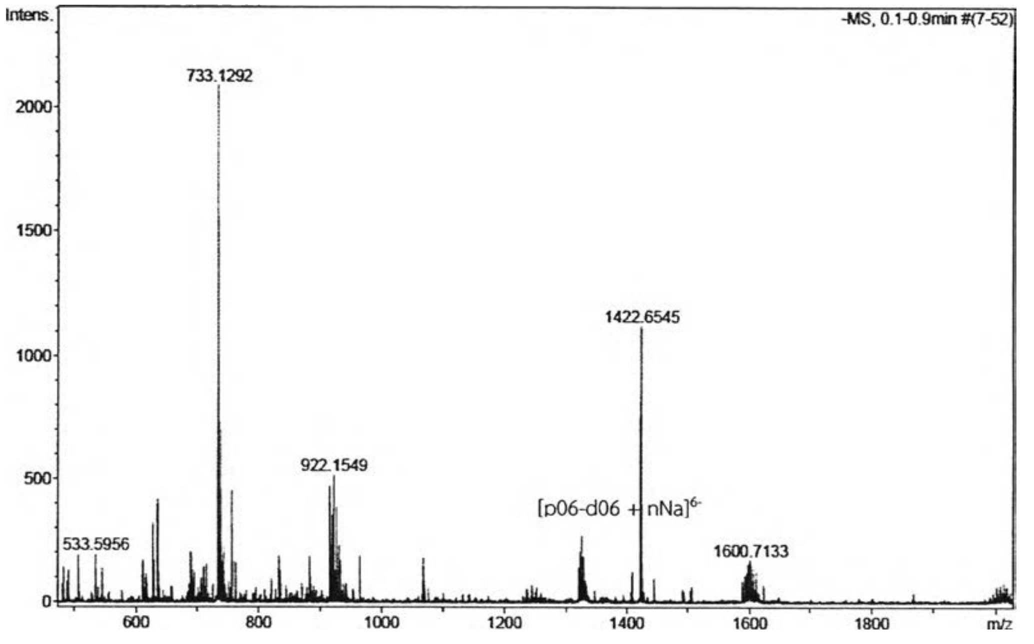

Figure A.190 Spectrum of duplex p06 - d06 at 20 eV.

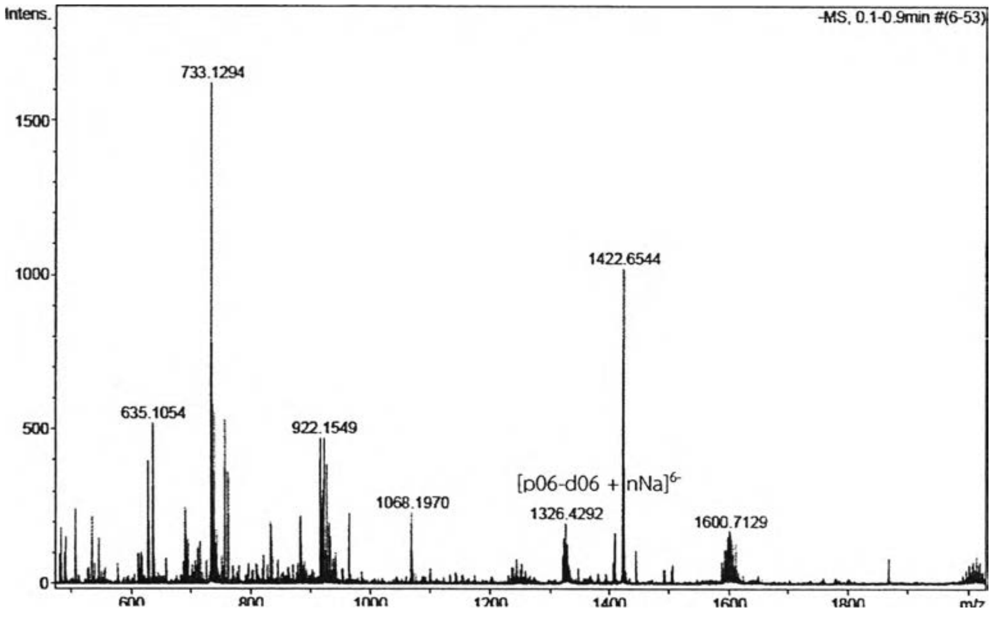

Figure A.191 Spectrum of duplex p06 - d06 at 22 eV.

Table A.1 Calculated E_{CM} values of duplex p01 (TT)-d01 (AA) by observe -6 charge.

	1			2			3		
E(Lab)	E(CM)	%Complex	%relative	E(CM)	%Complex	%relative	E(CM)	%Complex	%relative
0	0.0000	57.8900	87.9520	0.0000	37.5300	85.8417	0.0000	-	-
2	0.3523	52.2800	79.4287	0.3523	43.7200	100.0000	0.3523	55.9500	82.1948
4	0.7047	65.8200	100.0000	0.7047	38.7800	88.7008	0.7047	68.0700	100.0000
6	1.0570	61.4300	93.3303	1.0570	35.7000	81.6560	1.0570	48.0700	70.6185
8	1.4093	40.6700	61.7897	1.4093	22.7300	51.9899	1.4093	31.9600	46.9517
10	1.7617	25.8000	39.1978	1.7617	17.7200	40.5306	1.7617	26.3800	38.7542
12	2.1140	21.3800	32.4825	2.1140	17.2400	39.4328	2.1140	20.9300	30.7478
14	2.4663	25.3600	38.5293	2.4663	16.4300	37.5801	2.4663	23.4900	34.5086
16	2.8187	25.1800	38.2558	2.8187	16.9400	38.7466	2.8187	20.8900	30.6890
18	3.1710	23.7200	36.0377	3.1710	20.0600	45.8829	3.1710	23.1000	33.9357
20	3.5233	26.0300	39.5473	3.5233	20.4100	46.6834	3.5233	24.7100	36.3009
22	3.8757	20.4300	31.0392	3.8757	16.2400	37.1455	3.8757	21.4000	31.4382
24	4.2280	8.2400	12.5190	4.2280	10.7500	24.5883	4.2280	9.8200	14.4263

Table A.2 Calculated E_{CM} values of duplex p02 (AA)-d02 (TT) by observe -6 charge.

	1			2			3		
E(LAB)	E(CM)	%Complex	%relative	E(CM)	%Complex	%relative	E(CM)	%Complex	%relative
0	0.0000	15.3200	100.0000	0.0000	25.5700	100.0000	0.0000	23.1800	65.0758
2	0.3494	12.1900	79.5692	0.3494	14.3000	55.9249	0.3494	35.6200	100.0000
4	0.6988	10.8100	70.5614	0.6988	9.7000	37.9351	0.6988	22.9900	64.5424
6	1.0481	10.9300	71.3446	1.0481	9.1600	35.8232	1.0481	14.4300	40.5109
8	1.3975	10.2500	66.9060	1.3975	7.8400	30.6609	1.3975	12.5300	35.1769
10	1.7469	14.7300	96.1488	1.7469	9.1300	35.7059	1.7469	12.3600	34.6996
12	2.0963	9.8300	64.1645	2.0963	8.7100	34.0634	2.0963	10.3900	29.1690
14	2.4457	9.3600	61.0966	2.4457	7.9800	31.2084	2.4457	8.6300	24.2280
16	2.7950	8.5300	55.6789	2.7950	7.3500	28.7446	2.7950	9.2000	25.8282
18	3.1444	10.9300	71.3446	3.1444	7.2100	28.1971	3.1444	8.0600	22.6277
20	3.4938	8.1200	53.0026	3.4938	4.2400	16.5819	3.4938	6.7600	18.9781

Table A.3 Calculated E_{CM} values of duplex p03 (CC)-d03 (GG) by observe -6 charge.

	1			2			3		
E(Lab)	E(CM)	%Complex	%relative	E(CM)	%Complex	%relative	E(CM)	%Complex	%relative
0	0	30.66	100	0	28.1	93.01555776	0	22.8	60.19007392
2	0.349343097	25.08	81.80039139	0.349343097	30.21	100	0.349343097	37.88	100
4	0.698685854	20.65	67.35159817	0.698685854	20.33	67.29559748	0.698685854	26.65	70.35374868
6	1.04802672	16.7	54.46836269	1.04802672	20.16	66.73286991	1.04802672	16.8	44.35058078
8	1.397369943	12.46	40.63926941	1.397369943	12.19	40.35087719	1.397369943	12.75	33.65892291
10	1.746713744	9.31	30.3652968	1.746713744	13.51	44.72029129	1.746713744	10.2	26.92713833
12	2.096055984	9.49	30.95238095	2.096055984	10.84	35.88215823	2.096055984	8.96	23.65364306
14	2.445399123	9.59	31.27853881	2.445399123	9.82	32.50579278	2.445399123	8.83	23.31045407
16	2.794742947	10.79	35.19243314	2.794742947	12.19	40.35087719	2.794742947	7.93	20.9345301
18	3.144084052	8.25	26.90802348	3.144084052	9.97	33.00231711	3.144084052	9.11	24.04963041
20	3.493427149	8.68	28.31050228	3.493427149	6.65	22.01257862	3.493427149	7.9	20.85533263

Table A.4 Calculated E_{CM} values of duplex p04 (GG)-d04 (CC) by observe -6 charge.

	1			2			3		
E(Lab)	E(CM)	%Complex	%relative	E(CM)	%Complex	%relative	E(CM)	%Complex	%relative
0	0.0000	10.7400	84.9012	0.0000	8.3500	100.0000	0.0000	9.4100	96.8107
2	0.3493	12.6500	100.0000	0.3493	7.8900	94.4910	0.3493	9.7200	100.0000
4	0.6986	10.9600	86.6403	0.6986	5.9600	71.3772	0.6986	8.4800	87.2428
6	1.0479	9.4900	75.0198	1.0479	7.4900	89.7006	1.0479	7.9600	81.8930
8	1.3972	9.1000	71.9368	1.3972	6.4000	76.6467	1.3972	6.8300	70.2675
10	1.7465	8.4900	67.1146	1.7465	5.9900	71.7365	1.7465	6.7000	68.9300
12	2.0958	8.6300	68.2213	2.0958	5.9600	71.3772	2.0958	6.1000	62.7572
14	2.4451	9.8000	77.4704	2.4451	7.1400	85.5090	2.4451	5.7600	59.2593

Table A.5 Calculated E_{CM} values of duplex p05 -d05 by observe -6 charge.

	1			2			3		
E(Lab)	E(CM)	%Complex	%relative	E(CM)	%Complex	%relative	E(CM)	%Complex	%relative
0	0.0000	-	-	0.0000	-	-	0.0000	-	-
2	0.3491	8.7600	59.7137	0.3491	-	-	0.3491	9.2900	47.2053
4	0.6983	13.0200	88.7526	0.6983	5.2700	30.7110	0.6983	19.6800	100.0000
6	1.0474	14.0200	95.5692	1.0474	13.0800	76.2238	1.0474	18.6500	94.7663
8	1.3965	14.6700	100.0000	1.3965	17.1600	100.0000	1.3965	12.2200	62.0935
10	1.7456	12.3800	84.3899	1.7456	13.7100	79.8951	1.7456	9.5100	48.3232
12	2.0948	13.0700	89.0934	2.0948	9.8300	57.2844	2.0948	11.6900	59.4004
14	2.4439	14.0900	96.0464	2.4439	11.2800	65.7343	2.4439	13.2300	67.2256
16	2.7930	14.5800	99.3865	2.7930	12.8400	74.8252	2.7930	12.7100	64.5833
18	3.1422	12.5000	85.2079	3.1422	11.5200	67.1329	3.1422	14.3000	72.6626
20	3.4913	13.4100	91.4110	3.4913	14.3200	83.4499	3.4913	16.5100	83.8923
22	3.8404	11.8400	80.7089	3.8404	12.1400	70.7459	3.8404	11.0800	56.3008

Table A.6 Calculated E_{CM} values of duplex p06 -d06 by observe -6 charge.

	1			2			3		
E(Lab)	E(CM)	%Complex	%relative	E(CM)	%Complex	%relative	E(CM)	%Complex	%relative
0	0.0000	-	-	0.0000	-	-	0.0000	33.6300	100.0000
2	0.3511	-	-	0.3511	-	-	0.3511	24.7700	73.6545
4	0.7022	12.2600	79.4556	0.7022	10.8300	64.5796	0.7022	17.1400	50.9664
6	1.0533	13.6600	88.5288	1.0533	10.4700	62.4329	1.0533	12.9500	38.5073
8	1.4044	15.4300	100.0000	1.4044	13.4300	80.0835	1.4044	14.0300	41.7187
10	1.7554	12.2800	79.5852	1.7554	16.7700	100.0000	1.7554	10.4600	31.1032
12	2.1065	11.0400	71.5489	2.1065	14.9400	89.0877	2.1065	10.7900	32.0844
14	2.4576	13.3400	86.4550	2.4576	14.6800	87.5373	2.4576	10.7900	32.0844
16	2.8087	14.7600	95.6578	2.8087	15.3300	91.4132	2.8087	11.2400	33.4225
18	3.1598	13.4600	87.2327	3.1598	14.7100	87.7162	3.1598	10.5300	31.3113
20	3.5109	13.5000	87.4919	3.5109	15.7900	94.1562	3.5109	13.8400	41.1537
22	3.8620	11.7000	75.8263	3.8620	14.1400	84.3172	3.8620	12.0400	35.8014

Table A.7 Calculated E_{CM} values of duplex pT9 –dA9 by observing the -6 charge species.

E(Lab)	E(CM)	%Complex	%relative
0	0.0000	66.3600	79.9614
2	0.4664	82.9900	100.0000
4	0.9328	76.6500	92.3605
6	1.3992	54.4200	65.5742
8	1.8657	40.1300	48.3552
10	2.3321	23.2100	27.9672
12	2.7985	6.9300	8.3504
14	3.2649	1.3000	1.5665

VITA

Mr. Phubmodee Wichettapong was born on February 9th, 1988 in Khon Kaen, Thailand. He graduated Bachelor's Degree of Science, major in Chemistry from Faculty of Science, Chulalongkorn University, in 2010. He began studying his Master's degree at the Department of Chemistry, Faculty of Science, Chulalongkorn University in academic year of 2011.

His present address is 204 Moo 7, Tambon pharub , Amphoe Mueang, Khon Kaen, Thailand, 40000, e-mail : thai26675@gmail.com.